Available online at www.sciencedirect.com
SCIENCE DIRECT®
Deep-Sea Research I 53 (2006) 425–448
DEEP-SEA RESEARCH PART I
www.elsevier.com/locate/dsr

Enhanced ventilation in the Okhotsk Sea through tidal mixing at the Kuril Straits

Tomohiro Nakamura[a,*], Takahiro Toyoda[b], Yoichi Ishikawa[b], Toshiyuki Awaji[b,a]

[a]*Frontier Research Center for Global Change, JAMSTEC, Yokohama, 236-0001, Japan*
[b]*Department of Geophysics, Graduate School of Science, Kyoto University, Kyoto, 606-8502, Japan*

Received 25 October 2004; received in revised form 2 September 2005; accepted 27 December 2005

Abstract

The role played by tide-induced diapycnal mixing at the Kuril Straits in the formation of the Okhotsk Sea water is examined using an ocean general circulation model. The result shows that tidal mixing causes a freshening of intermediate water down to $\sim 27.6\sigma_\theta$. This implies an enhancement of ventilation by tidal mixing, since a freshening flux can come only from above in the Okhotsk Sea. In fact, when compared with the case without tidal mixing, the production rate of Dense Shelf Water (DSW) increases from 0.01 to 0.13 Sv ($10^6\,m^3\,s^{-1}$) with maximum DSW density increased from 26.6 to $26.8\sigma_\theta$. This enhanced production of DSW allows us to successfully reproduce a layer of local potential vorticity minimum in the Okhotsk Sea, which characterizes the Okhotsk Sea Mode Water. The analysis reveals that tidal mixing at the Kuril Straits has two roles in enhancing ventilation. First, it preconditions the water properties of the DSW because tidal mixing at the Kuril Straits induces an upward salt flux from the saltier lower layer. The subsequent transport of the saline water from the Straits to regions of sea-ice generation increases the density of subducting water, resulting in more realistic densities and production rates of DSW. Second, tidal mixing directly modifies water properties throughout the water column. The ventilation due to this mechanical mixing further enhances the intermediate layer ventilation, and is dominant in the Kuril Straits and in the layer denser than the DSW. Although the effect of double diffusion on ventilation in the Okhotsk Sea is also examined, it is much less effective than the tidal mixing. Since the Okhotsk Sea is a key location for the ventilation of the North Pacific intermediate layer, the important implication here is that tidal mixing at the Kuril Straits enhances the meridional overturning in the entire North Pacific Ocean.

Keywords: Tidal mixing; Subduction; Okhotsk Sea; North Pacific intermediate water

1. Introduction

The Okhotsk Sea, which is a marginal sea connected to the North Pacific Ocean through the Kuril Straits (Fig. 1a), has received much attention in association with ventilation of the North Pacific (e.g., Kitani, 1973; Favorite et al., 1976; Talley, 1991; Yasuda et al., 1996).

Observations show that Okhotsk Sea water is considerably different from the subarctic water of the North Pacific. In particular, the intermediate water in the Okhotsk Sea is considerably fresher, colder and more oxygenated than water at the same

*Corresponding author. Present address: Institute of Low Temperature Science, Hokkaido University, Sapporo 060–0819, Japan.
E-mail address: nakamura@lowtem.hokudai.ac.jp (T. Nakamura).

0967-0637/$ - see front matter © 2006 Elsevier Ltd. All rights reserved.
doi:10.1016/j.dsr.2005.12.006

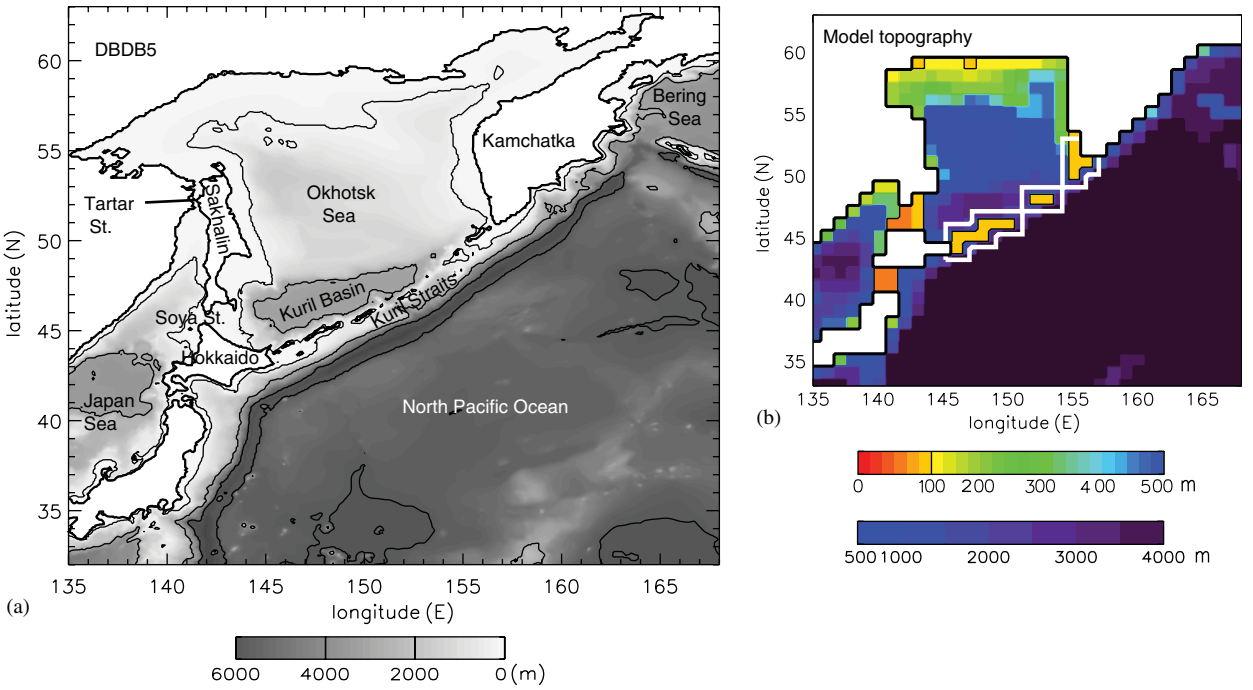

Fig. 1. (a) Bottom topography around the Okhotsk Sea. Contours are drawn at 200, 3000, and 6000 m depth. (b) Model topography around the Okhotsk Sea. Thick white lines indicate the region of enhanced vertical diffusion in the Tmix case, while thick black lines indicate land boundaries.

density in the subarctic Pacific and the difference extends to about 2000 m or 27.6σ_θ (Moroshkin, 1966; Yasuoka, 1968; Talley, 1991; Watanabe and Wakatsuchi, 1998; Freeland et al., 1998). Another important difference is the presence of a local maximum in the thickness of isopycnal layers around 26.8σ_θ, which is termed 'Okhotsk Sea Mode Water' (OSMW) (Yasuda, 1997).

These properties imply that ventilation signals in such layers are stronger in the Okhotsk Sea than in the subarctic Pacific. This fact means that ventilation in the Okhotsk Sea reaches the 27.6σ_θ density layer, and that it does not originate from the Pacific. Note that in the Okhotsk Sea, freshening below the surface layer is a good indicator of ventilation in much the same way as elevated oxygen concentrations. This is because salinity increases almost monotonically with depth around the Okhotsk Sea and because salinity values are lower in the Okhotsk Sea than in the North Pacific at the same potential density, and thus a freshening flux can come only from above. Also, a maximum in layer thickness usually indicates the influence of subduction as in the case of mode waters.

Supply of the Okhotsk Sea water modifies the subarctic water which flows as a western boundary current (East Kamchatka Current Water, EKCW). The modified water, called 'Oyashio water', spreads both to the subarctic and subtropic North Pacific (e.g., Favorite et al., 1976; Talley, 1991; Yasuda et al., 1996). In particular, the OSMW is considered to be a major source of the North Pacific Intermediate Water (NPIW) (Yasuda, 1997), which is characterized by a salinity minimum around 26.8σ_θ (Sverdrup et al., 1942). Because the NPIW spreads out over most of the subtropical gyre (Talley, 1993), the Okhotsk Sea is regarded as an important location for ventilation of the North Pacific intermediate layer. This view is also supported by observed distributions of Chlorofluorocarbons (CFCs) (Warner et al., 1996). Since the above ventilation process creates a body of water capable of storing large amounts of greenhouse gases such as CO_2 (e.g., Yamanaka and Tajika, 1996) as well as heat and fresh water, the clarification of the water-mass formation and subsequent transformation processes in the Okhotsk Sea is important for understanding, modeling, and predicting the potential response of the ocean to increased greenhouse gases and to long term variability in the North Pacific.

Within the Okhotsk Sea, the most important process in the transformation of the incoming

North Pacific water is considered to be sea ice production (e.g., Watanabe and Wakatsuchi, 1998). The associated brine rejection contributes to the production of highly saline water near freezing point observed over the shelf of the northern Okhotsk Sea (Kitani, 1973; Gladyshev et al., 2000). Note that this water is fresher than surrounding water at the same density since the water is close to the freezing point. The deeper component of this water, with a density greater than the winter mixed layer in the interior Okhotsk Sea (i.e., $>26.6\sigma_\theta$), is called 'Dense Shelf Water' (DSW). Its maximum observed density reaches $27.03\sigma_\theta$ (Kitani, 1973).

The production of the DSW freshens the intermediate layer, as the fresh DSW (and/or components derived from it through entrainment of the ambient water) is transported southward along the east coast of Sakhalin and into the Kuril Basin (e.g., Fujii and Abe, 1976; Talley, 1991). In the Kuril Basin, the fresh water originating from the DSW mixes widely with the water in the basin and thus ventilates the intermediate water of the Okhotsk Sea. This process includes the OSMW formation, which was traditionally thought to occur through isopycnal mixing of the DSW and the EKCW with a small contribution of Soya Warm Current Water (SWCW) (Yasuda, 1997; Watanabe and Wakatsuchi, 1998).

However, when compared with the DSW density ($\leqslant 27.05\sigma_\theta$), the ventilation signals in the Okhotsk Sea (i.e., the relatively fresh and oxygenated water) extends to much denser layers ($\sim 27.6\sigma_\theta$). Since the DSW is the densest water that is directly formed by surface forcing in both the North Pacific and the Okhotsk Sea (Talley, 1991; Gladyshev et al., 2000), diapycnal mixing of low salinity and high oxygen-content water from above must be working (though deeper subduction occurs in the Japan Sea, the shallow sills in the straits prevent it from leaking out). In fact, a result from a box model using CFCs in addition to potential temperature and salinity has suggested that diapycnal mixing is required for the production of the Okhotsk Sea water below $27.2\sigma_\theta$ (Wong et al., 1998). Also, an analysis of oxygen isotopes revealed that vertical mixing from above is also important in freshening of the Okhotsk Sea water even at the density of the DSW (Yamamoto et al., 2002). Hence, in order to better understand the water modification in the Okhotsk Sea, it is important to clarify the process responsible for such diapycnal mixing and the mechanism through which the mixing process affects the water mass structure.

Previous studies have underlined two possible mixing mechanisms. The first of these is tidal mixing in the Kuril Straits. Observations have found vertically mixed water in the Kuril Straits, down to $27.1\sigma_\theta$ or more (Kitani, 1973; Kawasaki and Kono, 1994; Gladyshev, 1995; Kawasaki, 1996). Locally enhanced ventilation is also indicated by the presence of a high oxygen anomaly in the Kuril Straits, which is observed from the surface to around 2200 m or $>27.4\sigma_\theta$ (Talley, 1991; Freeland et al., 1998). The high oxygen anomaly appears to intrude into the Okhotsk Sea on a deep $27.4\sigma_t$ surface (Yasuoka, 1968). By combining these facts, Kitani (1973) and Talley and Nagata (1995) suggested that diapycnal mixing in the Kuril Straits is responsible for water transformation in the Okhotsk Sea deeper than the DSW density layer. They further hypothesized that tidal mixing is the likely cause of the mixing. In fact, the tidal currents, especially the diurnal components, are very swift around the Kuril Straits with speeds exceeding $2\,\mathrm{m\,s^{-1}}$ in the relatively shallow straits (100–500 m depth) (e.g., Thomson et al., 1997; Talley and Nagata, 1995). Even in the deep Bussol Strait ($\sim$2000 m depth), the maximum speed exceeds $1\,\mathrm{m\,s^{-1}}$ (Katsumata et al., 2004; Nakamura and Awaji, 2004; Riser, 2001).

Recent modeling and theoretical studies (Nakamura et al., 2000a,b; Nakamura and Awaji, 2001, 2004) showed that the diurnal tides (especially the K_1 tide) have the ability to induce vigorous mixing (with a maximum diffusivity of over $1000\,\mathrm{cm^2\,s^{-1}}$). The mixing occurs from the surface to the sill bottom and across a wide area, thus causing large diapycnal transport to the deep layers. In these studies, the locally enhanced mixing is associated with tidally generated 'unsteady lee waves' rather than internal tides. This is because the diurnal tides are subinertial at the Kurils (so that internal-tides generated by them cannot be internal gravity waves) and because unsteady lee waves are more likely to grow by superposition than internal tides. Energetic internal waves are then formed with amplitudes exceeding 100 m in their simulations.

The second mechanism for enhanced diapycnal mixing is double diffusion (You et al., 2000). A situation favorable for diffusive double diffusion is found in the subarctic Pacific and the Okhotsk Sea. In these regions, salinity generally increases with depth, while temperature has a local minimum (called the dichothermal layer) just below the summer surface layer and a local maximum (the

mesothermal layer) below (e.g., Uda, 1963; Favorite et al., 1976). Thus, between the dichothermal and mesothermal layers, both temperature and salinity increase with depth, so that a necessary condition for diffusive double diffusion is satisfied. This situation develops at greater depth in the Okhotsk Sea ($\sim$26.8–27.2σ_θ) than in the North Pacific ($\leqslant$26.8σ_θ) (You et al., 2000), since the mesothermal layer in the Okhotsk Sea is much deeper than in the North Pacific (e.g., Yasuoka, 1968). Hence this mechanism could explain the deep ventilation in the Okhotsk Sea. However, it is not clear whether it is an important process for diapycnal mixing.

In this study, we investigate the effects of these two mixing processes on the ventilation of the Okhotsk Sea. To this end, a set of experiments using an OGCM is conducted with an emphasis on the role of tidal mixing at the Kuril Straits in modifying the Okhotsk Sea water, particularly in the production of the DSW. Our experiments suggest that tidal mixing is much more effective than double diffusion.

2. Model and experimental design

The model used is an OGCM developed at Kyoto University (Ishikawa et al., 2002; Nakamura et al., 2003a; Toyoda et al., 2004), which solves the primitive equations in spherical coordinates. For a realistic reproduction of subduction processes, this model adopts a third-order advection scheme for the tracer equation (UTOPIA and QUICKEST; Hasumi and Suginohara, 1999). In addition, the model incorporates isopycnal diffusion with eddy parameterization (Redi, 1982; Gent and McWilliams, 1990), together with a turbulence closure mixed layer scheme (Noh and Kim, 1999). In these schemes, both the isopycnal and the eddy-parameterization diffusivity coefficients are set to $10^7\,\mathrm{cm^2\,s^{-1}}$, and the background vertical and diapycnal diffusivity and viscosity coefficients are set to $0.01\,\mathrm{cm^2\,s^{-1}}$. To accurately simulate the subduction associated with brine rejection, a sea ice model is incorporated based on Ikeda (1989a,b). The sea ice model is a Hibler (1979) two-category ice model which solves ice momentum equations and the equations for ice concentration and ice volume (i.e., thickness times concentration). The effect of double diffusion is parameterized on the basis of Schmitt (1981) for the salt fingering condition and Fedorov (1988) for the diffusive convection condition, following Merryfield et al. (1999). Also, the partial cell method is used for a better representation of bottom topography. A more detailed description is given in Appendix A.

The model domain is nearly global (75°S–75°N), in order to simultaneously investigate the effect on the North Pacific (Nakamura et al., 2006). The horizontal resolution is $1^\circ \times 1^\circ$, and 34 levels are used in the vertical spaced from 20 m at the sea surface to 400 m, as shown in Table 1. The model topography is based on DBDB5 (U.S. National Geophysical Data Center) but care is taken not to smooth out the sills in the Kuril Straits (Fig. 1b), as discussed in Section 7. The initial values of potential temperature and salinity are taken from the World Ocean Atlas 1994 Monthly Data compilation (WOA94, Levitus and Boyer, 1994; Levitus et al., 1994). Sea surface fluxes are calculated with the bulk formulae (Röske, 2001; Ikeda, 1989b; da Silva et al., 1994), but the commonly used flux correction method is adopted for heat and fresh water fluxes with a relaxation time scale of 60 days (e.g., Barnier et al., 1995; Weaver and Hughes, 1996). The sensitivity to this method is discussed in Section 6. The atmospheric and river runoff data used are based on the climatological monthly mean data compiled by Röske (2001), which is in turn based on the European Centre for Medium-Range Forecasts reanalysis data. The ice and oceanic data used in calculating the surface fluxes are taken from simulated values, as is usual for an ice-ocean coupled model. In addition, restoration of potential temperature and salinity to those of WOA94 is

Table 1
Model vertical resolution

Level	Thickness (m)	Depth range (m)
1–3	20	0−60
4	25	60−85
5–6	30	85−145
7	35	145−180
8	45	180−225
9–10	50	225−325
11	60	325−385
12	75	385−460
13	90	460−550
14–16	100	550−850
17	125	850−975
18	150	975−1125
19	175	1125−1300
20	200	1300−1500
21–22	250	1500−2000
23–27	300	2000−3500
28–34	400	3500−6300

applied at the northern and southern boundaries, at the exits of the Mediterranean and Red Seas, and in layers deeper than 2000 m with the same time scale for flux correction. The Bering Strait is closed since water from the Arctic Ocean through the strait is not considered to affect the water mass formation in the North Pacific (e.g., Overland et al., 1994).

Three main experiments were conducted (Table 2) after a 40-year spinup by which time the model ocean had reached a state of approximate equilibrium. The first of these was a control experiment obtained by a further 40-year integration (hereafter the 'Ctrl' case). The second was an experiment for the case with tidal mixing (the 'Tmix' case). This case was obtained by a 40-year integration after the spinup, but with the vertical diffusivity coefficient over the sills at the Kuril Straits increased by $200\,cm^2\,s^{-1}$ (Fig. 1b), based on the results of Nakamura et al. (2000b) and Nakamura and Awaji (2004). Note that both the Ctrl and Tmix cases include the effect of double diffusion. To estimate its relative importance, a third experiment was conducted, which excludes double diffusion from the scenario simulated by the Tmix case (the 'noDD' case). In the Tmix and noDD cases, the flux correction was not applied around the Kuril Straits in order to avoid artificial heat and fresh water fluxes which would arise due to the fact that the WOA94 data does not resolve the vertically mixed water in the Kuril Straits.

Table 2
List of experiments

Case	Increase in Kz at the Kuril Straits	Double diffusion	Flux correction
Main experiments			
Ctrl	None	Included	60 days
Tmix (Kz200)	$200\,cm^2\,s^{-1}$	Included	
noDD	$200\,cm^2\,s^{-1}$	None	
Sensitivity experiments			
Kz10	$10\,cm^2\,s^{-1}$		
Kz20	$20\,cm^2\,s^{-1}$		
Kz30	$30\,cm^2\,s^{-1}$		
Kz50	$50\,cm^2\,s^{-1}$		
Kz100	$100\,cm^2\,s^{-1}$	Same as Ctrl case	
Kz200 (Tmix)	$200\,cm^2\,s^{-1}$		
Kz300	$300\,cm^2\,s^{-1}$		
Kz500	$500\,cm^2\,s^{-1}$		
Kz1000	$1000\,cm^2\,s^{-1}$		
FC30	Same as Tmix case		30 days

Vertical diffusivity coefficient, Kz, is specified over the sills in the Kuril Straits except for the Ctrl case. Double-diffusion parameterization is excluded only in the noDD case. The relaxation time of flux correction is set to be 60 days except for the FC30 case.

It should be noted that tides were not directly simulated and their effect was parameterized through local increase of vertical diffusion, which is important particularly on the scales under consideration (e.g., Shiller et al., 1998; Hibiya et al., 1998). Although the tidal motion has other important effects, the present study focuses only on the effects of enhanced vertical mixing to gain a basic insight into one of the major tidal effects before exploring more comprehensive and thus more complicated effects. Also, the value of vertical diffusion is increased at all depths in the Kuril Straits as a first approximation. Strong tidal mixing reaches the surface layer from the bottom in the Kuril Straits, according to ship and satellite observations and tidal simulations (e.g., Kawasaki, 1996; Gladyshev, 1995; Kawasaki and Kono, 1994; Nakamura and Awaji, 2004). The specified value ($200\,cm^2\,s^{-1}$) roughly corresponds to twice that induced by the K_1 tide (Nakamura and Awaji, 2004). The reason for this selection is that the total tidal flow speed in the Kuril Straits is roughly twice as large as that of the K_1 component alone, according to the tidal simulations reported by Nakamura et al. (2000a). Taking this fact into account, the above rough estimate of diapycnal diffusivity was used for a basic investigation of the impacts of tidal mixing on the Okhotsk Sea.

In order to examine the sensitivity of the water modification in the Okhotsk Sea to the strength of the tidal mixing, eight experiments were additionally conducted, in which the increase in vertical diffusivity coefficient was varied from 10 to $1000\,cm^2\,s^{-1}$ (Kz10–Kz1000 cases, respectively). Also, for the discussion on the sensitivity to the flux correction method, another experiment was performed, in which the relaxation time scale was changed to 30 days while the other settings were the same as in the Tmix case (FC30 case). The settings used in all of our experiments are summarized in Table 2.

In the analysis below, the final year of the integration (i.e. the 80th year) is used. The sensitivity experiments for both the tidal mixing and the flux correction will be discussed in Section 6.

3. Circulation and sea ice in the Ctrl case

Prior to a comparison between the main experiments made in Section 4, the performance of the

OGCM in the Ctrl case is discussed in this section in terms of water circulation and sea ice formation in and around the Okhotsk Sea.

3.1. Current field

Fig. 2a shows near surface current fields in summer and winter around the Okhotsk Sea in the Ctrl case. In general, the simulated large-scale circulations in both basins reasonably reproduce the familiar gross features. For example, the large-scale cyclonic circulation in the Okhotsk Sea, the subarctic and subtropic gyres in the North Pacific, and the western boundary currents (i.e., the East Kamchatka Current (EKC), the Oyashio, and the Kuroshio) simulated here are basically consistent with both past observational studies (e.g., Favorite et al., 1976) and a recent state estimation by data assimilation (Awaji et al., 2003).

A detailed examination of Fig. 2a in the Okhotsk Sea shows that the simulated current field qualitatively reproduces the following important features of the intermediate water formation. Based on temperature and salinity observations it is inferred that relatively warm water flows into the Okhotsk Sea from the North Pacific mainly through the northern passages of the Kuril Islands (e.g., Kitani, 1973; Favorite et al., 1976). The inflowing water flows northward, forming the eastern part of the cyclonic circulation. On the other hand, the western part of the cyclonic circulation consists of the East Sakhalin Current (ESC), whose presence has been recently confirmed from mooring observations (Ohshima et al., 2002; Mizuta et al., 2003). This southward part of the circulation carries the water transformed in the northern Okhotsk Sea to the Kuril Basin, and eventually to the Pacific mainly through the central part of the Kuril Islands. In addition, an inflow from the Japan Sea through the shallow Soya Strait (40 m) brings the SWCW, which flows southwestward along the coast of Hokkaido with part of it diffusing into the Kuril Basin before flowing out of the Okhotsk Sea. These current features are also seen in Fig. 2a, though the Soya Warm Current (SWC) is difficult to identify in the March period due to its seasonal variation (discussed in the next section).

3.2. Volume transport

Given the qualitative similarity between the simulated and observed current field, we made a quantitative comparison of the volume transports of the main currents around the Okhotsk Sea—namely, the EKC and Oyashio in the North Pacific and the SWC and ESC in the Okhotsk Sea. (Volume transport is chosen here because model results represent spatially averaged fields on a grid scale, and hence observed values should be also averaged or integrated for a proper comparison. Observations in the other regions of the Okhotsk Sea are too limited for this purpose.)

The calculated monthly volume transports are shown in Fig. 3. The phases of the transports of these currents are consistent with observational studies and their amplitudes are also reasonable (e.g., Talley and Nagata, 1995; Kono and Kawasaki, 1997; Aota and Kawamura, 1978; Mizuta et al., 2003). In particular, the range of the calculated SWC transport (0.3 Sv in winter and 1.2 Sv in summer) is in good agreement with observational estimates of 0.1 Sv in winter and 1.2 Sv in summer (Aota and Kawamura, 1978; Matsuyama et al., 1999; Itoh et al., 2003). The reason for such a good agreement is that the driving force of the SWC is associated with the difference in sea surface height between the Okhotsk Sea and the Japan Sea, which in turn is associated with a large scale wind and thus is reasonably reproduced.

Most of the other transports are also within the range of observational estimates, as summarized in Table 3 (e.g., Reid, 1973; Talley and Nagata, 1995; Yasuda et al., 2001, 2002; Kono and Kawasaki, 1997; Shimizu and Ohshima, 2002; Ohshima et al., 2002; Mizuta et al., 2003). The simulated EKC transport is in good agreement with most observational estimates (Table 3). Although the summertime Oyashio transport in the Ctrl case is somewhat small, this is partly due to the absence of a tidal mixing effect (the transport increases by 1–3 Sv in the Tmix case) and because of the somewhat coarse resolution. The latter makes the simulated Oyashio more closely subject to the Sverdrup transport as compared with observations, which in turn results in a northward shift of its separation latitude when compared with the observations and thus leads to a smaller summertime transport off Hokkaido Island. The simulated ESC transport (1.0–2.8 Sv) is considerably smaller than the estimated transport based on mooring observations (1.2–12.3 Sv), which is considerably larger than the Sverdrup transport (and/or that expected from the wind stress and the linear wave dynamics, Shimizu and Ohshima, 2002) in winter. Because the volume transport due to

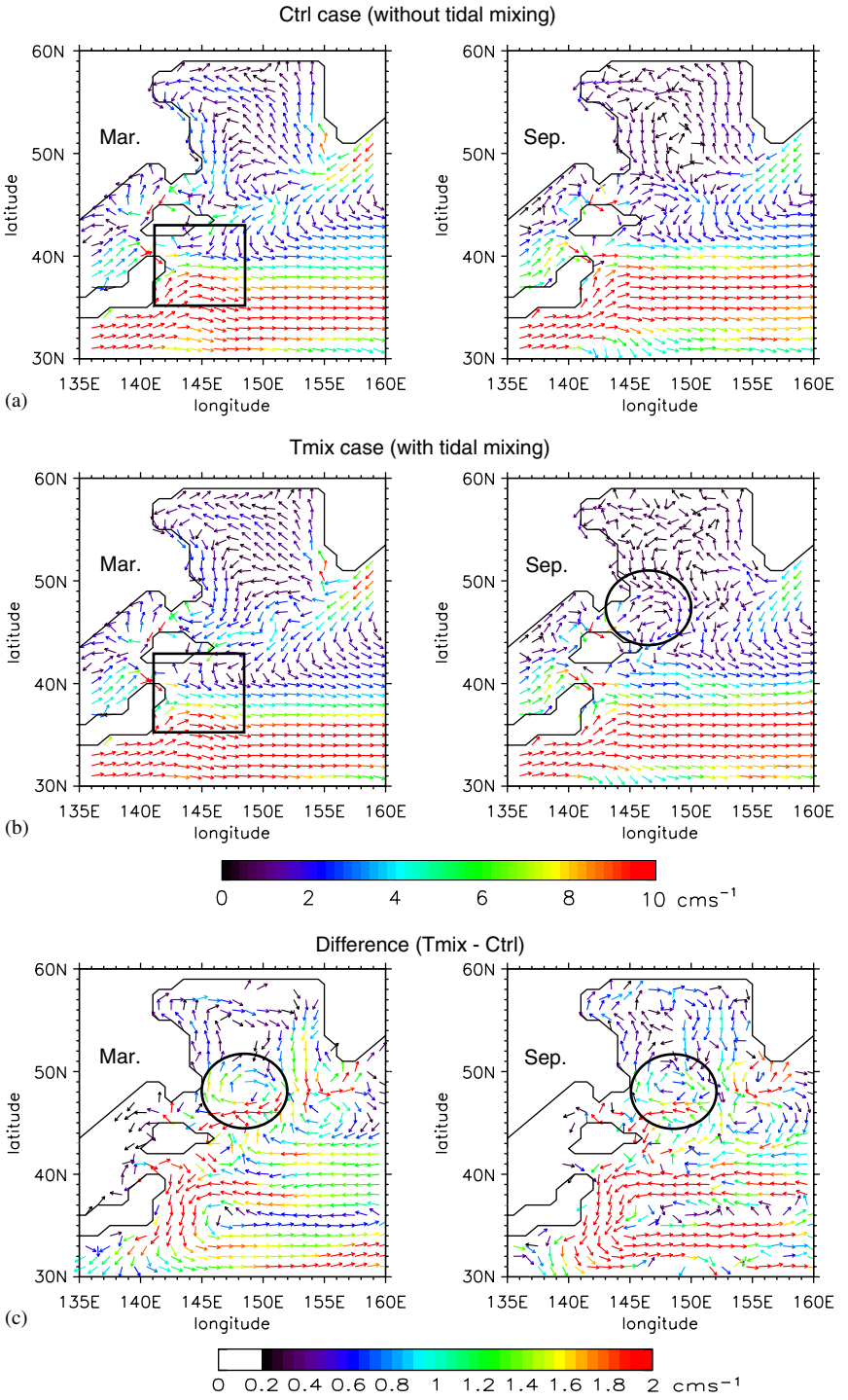

Fig. 2. Velocity vectors at 50 m depth of (a) Ctrl and (b) Tmix cases and (c) their difference in winter (left) and summer (right). The circles in panels (b) and (c) indicate the anticyclonic gyre strengthened by tidal mixing, and squares in panels (a) and (b) indicate the southward shift of the separation latitude of both the Oyashio and Kuroshio due to tidal mixing.

thermohaline forcing is not significant (Mizuta et al., 2003), the difference between the Sverdrup transport and the estimate from the mooring observation could arise from effects of recirculation or eddies. Since these effects are not resolved well in our model, the simulated volume transport is closer

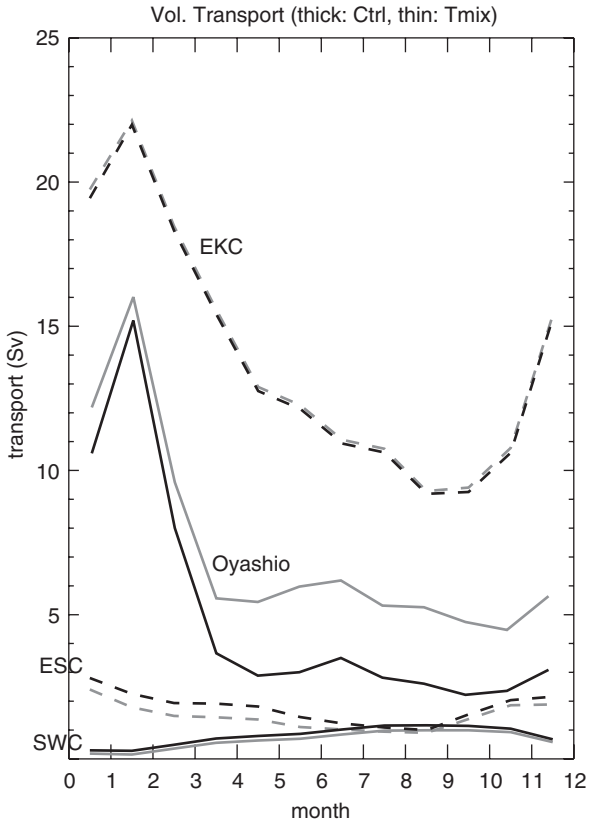

Fig. 3. Monthly volume transports of the Soya Warm Current (SWC) and the East Sakhalin Current (ESC) in the Okhotsk Sea, and the East Kamchatka Current (EKC) and the Oyashio in the North Pacific in the Ctrl (thick) and Tmix (thin) cases. These transports are calculated as follows; the SWC is calculated as an eastward transport through the Soya Strait, the ESC as a southward transport at 51.5°N in the western part of the Okhotsk Sea, the EKC as a westward transport at 158.5°E between the Kamchatka Peninsula and 42.5°N, and the Oyashio as a southward transport at 43.5°N between the Hokkaido Island and 155.5°E.

Table 3
Comparison of volume transport

Observational estimates	EKC	Oyashio	SWC	ESC
Summer or fall	~10	2–10	1.2 (max)	−0.2–4
Winter or spring	20–25	10–21	0.1 (min)	1.2–12.3
Ctrl case (max or min)				
Summer or fall	9	2	1.2	1.0
Winter or spring	22	15	0.3	2.8

The references for observational estimates are provided in the text. For acronyms and the calculation method of simulated vales, please refer to the caption of Fig. 3.

to the Sverdrup transport. Nevertheless, qualitative similarities suggest that our results would be reasonable in a qualitative sense.

The above qualitative and quantitative similarities suggest that the OGCM reasonably reproduced the observed flow field at least on a basin scale (the Okhotsk Sea scale), although some aspects of the ocean circulation, particularly those driven by thermohaline forcing, are not well presented in the Ctrl case due to the lack of tidal mixing, as discussed in Section 4.1.

3.3. Sea ice

In addition to circulation, a reasonable production of sea ice is also required for realistic investigations of subduction in the Okhotsk Sea. Fig. 4 shows the monthly averaged distributions of ice concentration and thickness simulated by the sea ice model in the Ctrl case.

The simulated ice distribution was basically similar to the observed ones. Sea ice begins to form along the northern coast of the Okhotsk Sea usually in December and then spreads southward due mainly to strong winds to cover both the northern and western coasts. Ice volumes and areas reach maxima in March, and more than a half of the Okhotsk Sea is covered (as is observed in usual winter). Such active ice formation mainly occurs in coastal polynyas along the northern shelf of the Okhotsk Sea. The ice gradually retreats northward, and almost disappears around the end of May. These main features are seen both in simulations and in observations (e.g., JMA, 2003; Alfultis and Martin, 1987; Martin et al., 1998; Cavalieri et al., 2002; Fetterer and Knowles, 2002), though the commencement of ice growth is somewhat delayed in the model.

Quantitatively, the simulated value of ice production in the Ctrl case ($2.1 \times 10^{11}\,m^3$) is nearly equal to a 12-year average of observational estimates ($2.27 \times 10^{11}\,m^3$) calculated from the reports of Alfultis and Martin (1987), Martin et al. (1998), and Gladyshev et al. (2000) and is well within the observed variability ($1.2–3.4 \times 10^{11}\,m^3$). Thus, the amount of brine rejection is also reasonably reproduced. Despite this good agreement, the simulated value of the maximum ice-covered area ($4.5 \times 10^5\,km^2$) is smaller than the observed value of a usual winter ($11 \times 10^5\,km^2$, JMA 2003). This may, in part, be due to the fact that the model Okhotsk Sea does not include the very shallow part of the

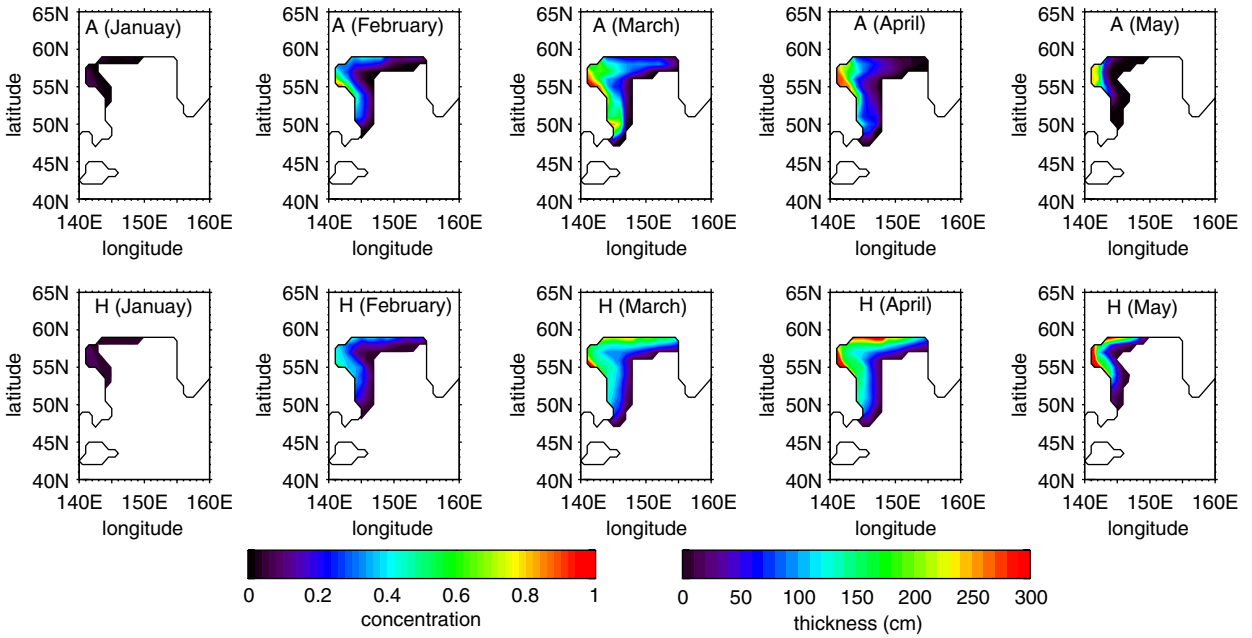

Fig. 4. Monthly distributions of ice concentration (upper) and thickness (lower) in the Ctrl case from January to May.

Shelikov and Shantarskiy Bays and because the SWC transport is somewhat large in winter, so that some melting takes place around Hokkaido Island.

Such qualitative and quantitative similarities in sea ice formation as well as water circulation confirm our basic approach to the investigation of tidal mixing effects in the Kuril Straits in water mass modification within the Okhotsk Sea.

4. Changes in water mass structure

Effects of tidal mixing and double diffusion on ventilation are now examined by comparing the Ctrl, Tmix, and noDD cases. Fig. 5 shows the salinity, potential temperature (θ), and potential vorticity (PV) fields for the three cases and for the WOA94 field in a meridional section across the western part of the Okhotsk Sea, where the water transformed in the Okhotsk Sea is most visible (PV is here calculated from $(f+\zeta)/\rho \times (\partial\sigma_\theta/\partial z)$, where ρ is potential density and ζ is relative vorticity). The differences of salinity and potential temperature from the Ctrl case are also shown in Fig. 6.

4.1. Impact of tidal mixing

Comparison of the Ctrl and Tmix cases suggests that the addition of tidal mixing significantly changes the simulated water mass structure. When compared with the Ctrl case, both salinity and potential temperature values in the Tmix case decrease considerably in the intermediate layer of the Okhotsk Sea, down to $\sim 27.6\sigma_\theta$ or 1500 m depth (Fig. 6), and thereby become much closer to the observed distributions (Fig. 5). The maximum decrease exceeds 0.4 for salinity and 2 °C for potential temperature in the intermediate layer (Fig. 6).

Since salinity principally determines the density variation in the subarctic Pacific and the Okhotsk Sea, an improvement in the representation of salinity distribution implies an improved density structure. Also, the cooling of the intermediate layer results in the weakening of the local temperature maximum (the mesothermal layer) in the Okhotsk Sea as compared with the Ctrl case (and the subarctic water). This mesothermal layer is a marked feature of the subarctic Pacific water, and its weakening is one of the characteristic features of the Okhotsk Sea (e.g., Kitani, 1973).

It is noteworthy that a local PV minimum in the vertical direction is produced in the Tmix case in the Okhotsk Sea around 300–500 m depth (Fig. 5), whereas it is absent in the Ctrl case (although a weak minimum can be seen, its saline and warm nature implies that it is not created in the Okhotsk Sea). This feature is similar to that observed by Freeland et al. (1998), and its presence here is

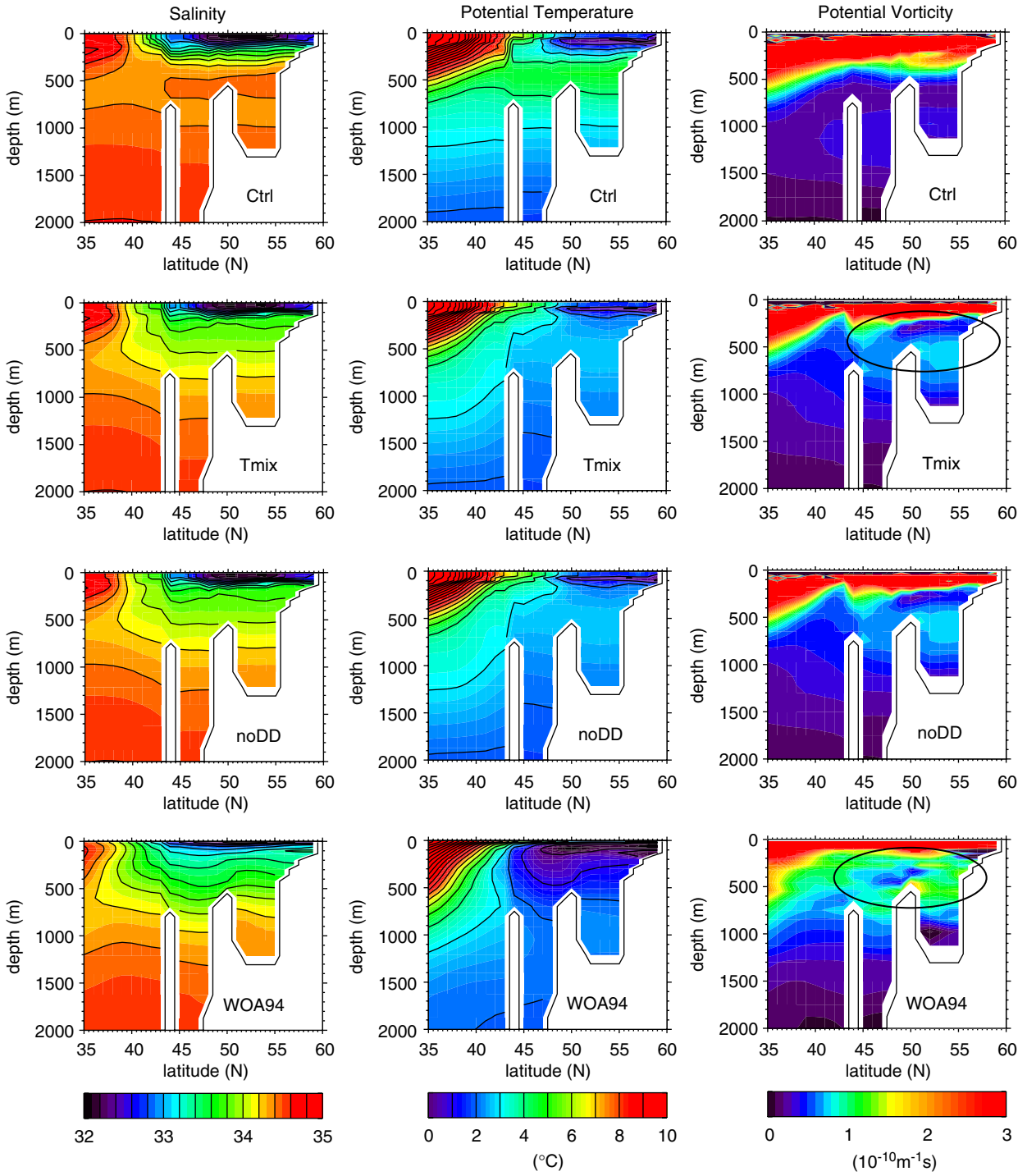

Fig. 5. Annual mean salinity, potential temperature and potential vorticity along 145°E for the Ctrl (top), Tmix (upper middle), and noDD (lower middle) cases and WOA94 (bottom). Circles in the potential vorticity field indicate the local minimum mentioned in the text.

remarkable since it is a characteristic feature of the OSMW. (On these horizontal scales, a local minimum in PV in the vertical direction roughly corresponds to a local maximum in layer thickness, which is an important feature of the OSMW.) In addition, qualitative features of the seasonal varia-

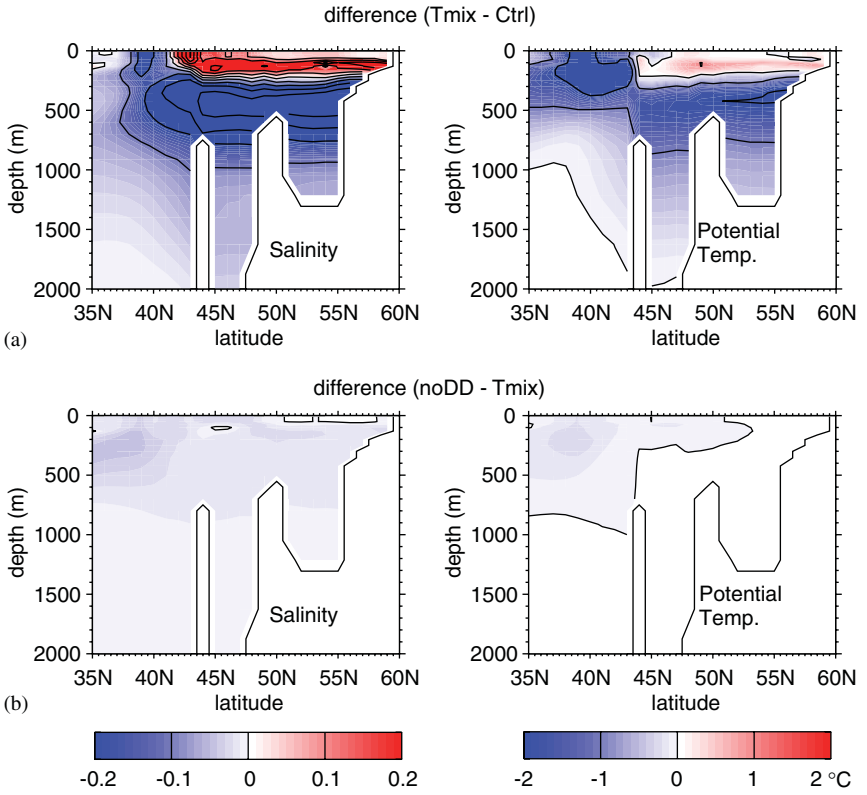

Fig. 6. Differences of salinity and potential temperature in Fig. 5 between the Ctrl and Tmix cases (upper), and those between the Tmix and noDD cases (lower).

tion of the OSMW are basically consistent with those reported by Gladyshev et al. (2003). For example, temperature becomes relatively high in summer to fall and low in winter to spring (not shown), although the reproduction of detailed and/or quantitative features needs further improvements.

From the viewpoint of ventilation, the enhanced freshening below the surface layer implies enhanced ventilation as noted in the introduction. One reason for the enhanced ventilation is the enhancement of subduction, which is suggested by the production of the PV minimum water. (Subduction here means the direct sinking of surface water.)

The enhanced subduction is confirmed by an increase in the production rate of the DSW as compared with the Ctrl case (Table 4). The DSW is defined here as $\theta < -1\,^{\circ}\mathrm{C}$, $\sigma_\theta \geqslant 26.6$, following Gladyshev et al. (2000). Using this definition, an annual mean production rate was estimated as the maximum amount of the DSW over a 1 year period, since the DSW disappears before the following winter (in both the model results and observations).

Table 4
Production rate and density of DSW and ice volume

Case	DSW production rate	DSW maximum density	Ice production
Ctrl	0.01 Sv	$26.6\sigma_\theta$	$2.1 \times 10^{11}\,\mathrm{m}^3$
Tmix	0.13 Sv	$26.8\sigma_\theta$	$2.3 \times 10^{11}\,\mathrm{m}^3$
Obs.	0.2–0.67 Sv	$27.0\sigma_\theta$	$1.2\text{–}3.4 \times 10^{11}\,\mathrm{m}^3$

The DSW is defined as $\theta < -1\,^{\circ}\mathrm{C}, \sigma_\theta \geqslant 26.6$. The references for observational estimates are provided in Section 3.3.

The annual mean production rate in the Ctrl case (0.01 Sv) is negligible, whereas the rate in the Tmix case (0.13 Sv) is one order of magnitude larger than that in the Ctrl case and is around the range of observational estimates (Martin et al., 1998; Gladyshev et al., 2000; Itoh et al., 2003).

On the other hand, the freshening (and thus ventilation) extends to deeper layers than the PV minimum layer (Figs. 5 and 6), as in the observations. Since the ventilation of the layers denser than the DSW (or the PV minimum) cannot be caused by

subduction, it must therefore be caused by vertical mixing. In this case, the latter is due to the tidal mixing. Tidal mixing therefore dictates the water properties of the upper intermediate layer by enhancing subduction (together with its direct mixing effect), and influences the denser layers through direct mixing only.

Associated with these changes, the circulation is also modified in the Tmix case (Figs. 2b and c). For example, an anticyclonic gyre in the Kuril Basin is strengthened in summer (circled in Fig. 2) by the PV supply due to both the enhanced subduction and tidal mixing at the Kuril Straits. In the intermediate layer, such seasonal variability also appears in the Tmix case, whereas it is almost absent in the Ctrl case (not shown). These features of the Tmix case are in agreement with the observation reported by Wakatsuchi and Martin (1991). Thus, we conclude that tidal mixing in the Kuril Straits is also important for driving the circulation in the Kuril Basin, where wind-driven circulation is relatively weak (Sekine, 1990; Shimizu and Ohshima, 2002).

4.2. Impact of double diffusion

In contrast, water properties in the Tmix and noDD cases are almost the same, as seen in Figs. 5 and 6. This implies that the diapycnal mixing due to double diffusion is too weak to modify the water mass structure in the presence of the tidal mixing effect. Also, the double diffusion effect does not cause deep ventilation and associated freshening in the absence of the tidal mixing effect, as seen in the Ctrl case. These results suggest that double diffusion is ineffective in ventilating the Okhotsk Sea regardless of the presence of the tidal mixing.

This is consistent with an expectation based on the typical value of the density ratio, $(\alpha/\beta)(dT/dS)$, where α and β are the thermal expansion and haline contraction coefficients of seawater at given temperature and salinity values, and dT and dS are the vertical changes at a given point in the water column. The estimated density ratio is about 0.2 in the density range between $26.8\sigma_\theta$ and $27.3\sigma_\theta$ using the climatological vertical profile of dT and dS in the Kuril Basin taken from Watanabe and Wakatsuchi (1998). Thus the vertical diffusivity coefficient due to double diffusion is estimated to be about $0.3\,cm^2\,s^{-1}$ (e.g., Zhang et al., 1998) and would thus be much smaller than that due to tidal mixing.

It should be noted that in the Okhotsk Sea, tidal currents are strong in both speed and shear, so the simple double diffusion parameterization used here probably includes some uncertainty. Nevertheless, if the double diffusion process is not drastically intensified by such strong currents, the above results would qualitatively hold. It is thus likely that tidal mixing in the Kuril Straits is the primary cause of the enhanced ventilation observed in the Okhotsk Sea.

5. Mechanism of the enhanced subduction

Although the above results revealed that tidal mixing enhances the ventilation in the Okhotsk Sea through both direct mixing and the enhancement of subduction, the mechanism of the enhanced subduction is not apparent.

To clarify this mechanism, we first compared the sea ice production between the two cases (Table 4) since the DSW is traditionally thought to have been formed by brine rejection. However, the difference in the sea ice production is only 10% and is not significant. This is because the production rate of sea ice is mainly determined by heat and momentum fluxes at the sea surface, which are almost the same in the two cases. Thus, the difference in the amount of brine rejection is negligible, as compared with the huge difference in the DSW production rate. This fact implies the presence of some other important controlling factor in the DSW production.

We then examined the seasonal change in the θ–S diagram in the Okhotsk Sea except for the Kuril Straits (Fig. 7). In the Ctrl case, comparison of summer and winter regimes indicates that seasonal variability due to summer heating and winter cooling is limited to about the $26.4\sigma_\theta$ density layer, which becomes the temperature minimum layer in summer (i.e., the bottom of the seasonal thermocline). Although brine rejection augments the production of denser water near the freezing temperature, subduction reaches at most the $26.6\sigma_\theta$ density layer. Accordingly, layers denser than the subducted water ($26.6\sigma_\theta$) show little seasonal variation (Fig. 7) and are not significantly transformed from the subarctic Pacific water (Fig. 5). This leads to the presence of warmer and saltier intermediate water in the Okhotsk Sea when compared with observations.

In the Tmix case, diapycnally mixed water appears below the seasonal thermocline in summer. The mixed water can be identified from a comparison of the θ–S diagrams of the Ctrl and Tmix cases in summer (Fig. 8a). In the density range lighter

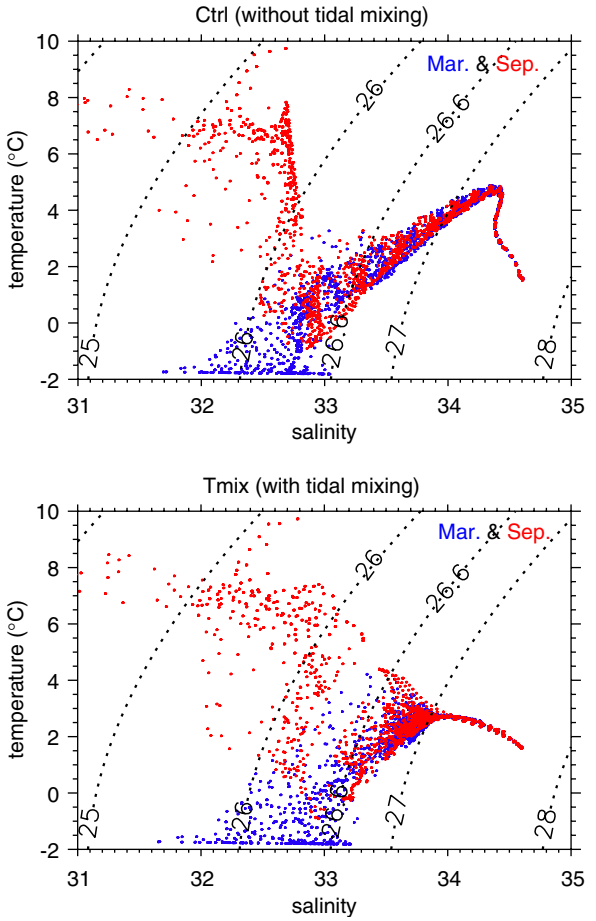

Fig. 7. θ–S diagrams in the Okhotsk Sea except near the Kuril Straits for the Ctrl (upper) and Tmix (lower) cases in winter (blue dots) and summer (red dots).

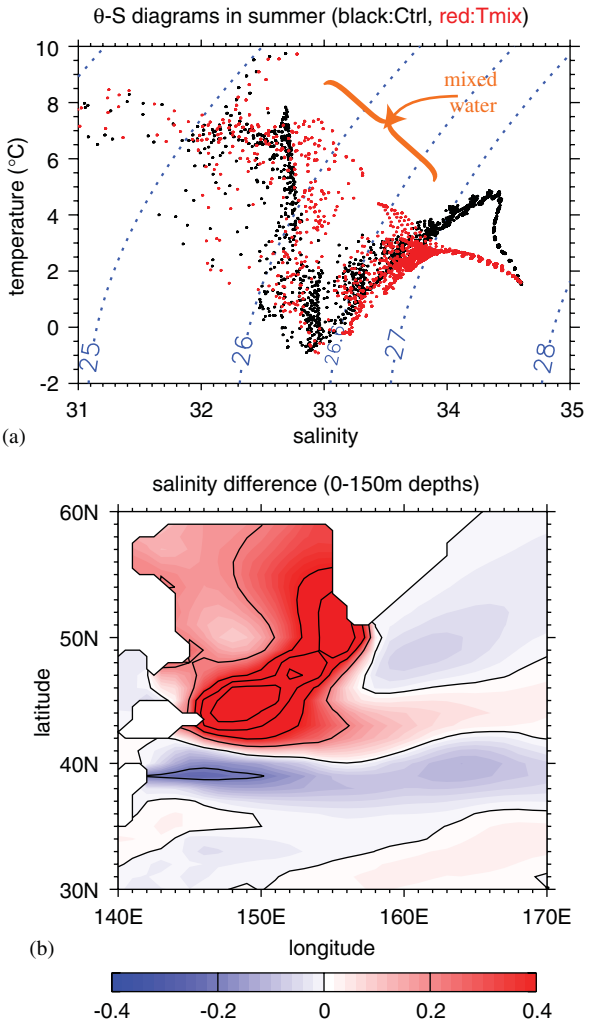

Fig. 8. (a) Comparison of the θ–S diagrams of the Ctrl (black dots) and Tmix (red dots) cases in summer. (b) Map of the salinity difference between the Ctrl and Tmix cases in the summer surface layer (upper 150 m).

than 27.0σ_θ, the θ–S plots in the Ctrl case (black dots) show a V-shape distribution with the bottom of the V-shape corresponding to that of the seasonal thermocline, while those in the Tmix case (red dots) are also present in the interior of the V-shape. We can approximately regard the water located in the interior of the V-shape in Fig. 8a as diapycnally mixed water for the following reason. The water warmed by summer heating from above (i.e., raised in θ–S diagram) is lighter than that at the bottom of the seasonal thermocline (and should be aligned along the seasonal thermocline). Hence, as the water in the interior of the V-shape cannot be produced by summer heating it should be produced by diapycnal mixing, which is due to tidal mixing at the Kuril Straits in this case.

The mixed water in the interior of the V-shape (and/or near the surface) is saltier at the same density than the water that is not affected by the tidal mixing (or water in the Ctrl case), that is, the vertical mixing at the Kuril Straits induces upward salt flux from the saltier lower layer. Such saline mixed water originating in the Kuril Straits is transported northward by the large-scale cyclonic circulation. In fact, a map of the salinity difference in the summer surface layer (upper 150 m) shows that the saltier water in the Kuril Straits extends along the eastern boundary of the Okhotsk Sea and to the northern coast, where the DSW forms (Fig. 8b).

Cooling of this saltier water in winter (together with brine rejection) enables the subduction process

to produce the DSW at much more realistic rates and densities (maximum value $\sim 26.8\sigma_\theta$). In other words, the extra controlling factor of the DSW production discussed above is, in effect, a preconditioning, in which salinity values in the (near) surface layer increase enough to create the DSW. Note that although the increase in sea surface salinity leads to an increase in the amount of brine rejection, the difference in salt production would be only a few percent even when salinity values increase by 1. This is because an increase of 1 in sea surface salinity corresponds to only a few percent increase in proportion to the total values, which are around 30 (and because the salt production due to brine rejection depends on the total value). Hence, this preconditioning works mainly by increasing water density (due to salinity change) at the beginning of winter.

The newly formed DSW is transported southward to the Kuril Basin. Subsequently, isopycnal mixing of the DSW with its surroundings, especially with vertically well-mixed water in the Kuril Straits, freshens and cools the intermediate water. The vigorous tidal mixing at the Kuril Straits diffuses the subducted water further down, so that a layer denser than the DSW is freshened and cooled (Fig. 7). As a result, the θ–S curve in and below the intermediate layer becomes much flatter than that in the Ctrl case (Fig. 8a), and lies closer to the observed curve (Fig. 9). This feature is one of the major characteristics of Okhotsk Sea water.

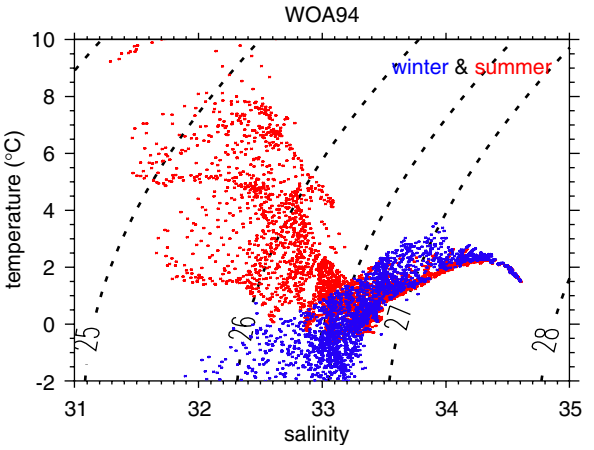

Fig. 9. θ–S diagrams in the Okhotsk Sea except near the Kuril Straits for WOA94 in winter (blue dots) and summer (red dots).

6. Sensitivity to tidal mixing and flux correction

In this section, we examine the sensitivity of our results to the strength of tidal mixing in the Kuril Straits and to the restoring time scale of the flux correction method.

For the former, we focus, particularly, on the DSW production. Both the production rate and the maximum density of the DSW are sensitive to the tidal mixing and generally increase with increasing tidal mixing strength (Fig. 10a,b). The production rate in the Kz10 to Kz1000 cases becomes 5 to 80 times larger than that in the Ctrl case, and the maximum DSW density in these cases increases by 0.06 to $0.3\sigma_\theta$ from that in the Ctrl case. In contrast, ice production is roughly constant (Fig. 10c). The difference from the Ctrl case is less than 20% for the range of vertical diffusion values. (The ice production increases slightly with increasing mixing. This is possibly because sea surface temperature is slightly lowered in summer and fall due to diapycnal mixing with the cold dichothermal layer, i.e., the remnant of the winter mixed layer.) Hence, in all the cases, enhanced production of DSW is not driven by change in sea ice production but by increase in salinity of the surface water caused by increased diapycnal mixing.

Accordingly, although the strength of tidal mixing should be estimated more precisely by future observations, the mechanism identified in this study will be valid at least for the above range of tidal mixing strength. In fact, the mechanism requires only two features in addition to vertical mixing at the Kuril Straits and winter cooling. That is (i) the fresher surface layer due to the large fresh water flux, and (ii) water transport from the Kuril Straits to the northern shelf of the Okhotsk Sea, which is conducted by the clockwise circulation in this case (and could be augmented by eddy or wave induced transport). These features are seen in both the model results and observations. The mechanism will thus be quite robust, at least qualitatively.

When compared with observations, the change in ice volume is within 12% of the observed 12-year average, considerably less than the amplitude of the observed interannual variation (about 50%). On the other hand, the production rate and maximum density of the DSW are somewhat less than the observational estimates. The possible reasons for the underestimates are two fold. One is the use of a coarse-resolution hydrostatic-model, which could generally result in weaker convection. This is because of insufficient resolution of bottom topography (which lacks for example the canyon effect),

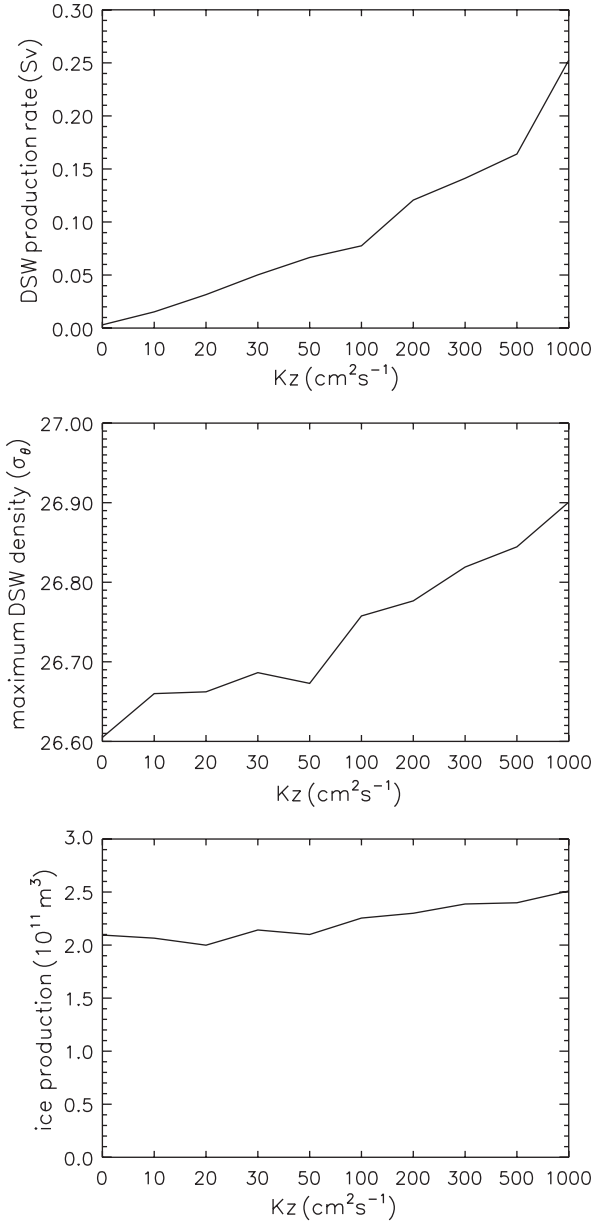

Fig. 10. (a) DSW production rate, (b) the maximum DSW density, and (c) ice production in the Okhotsk Sea as a function of the vertical diffusivity coefficient (Kz) specified in the Kuril Straits. Kz = 0 and Kz = 200 correspond to the Ctrl and Tmix cases, respectively. The DSW is defined as $\theta < -1\,^{\circ}\mathrm{C}, \sigma_\theta \geqslant 26.6$.

unresolved patchy convection, or absence of non-hydrostatic effect (which could cause a downdraft). The other is an underestimate of salination, which could in turn arise from an underestimate of tidal mixing and/or errors in fresh water flux. In addition, satellite derived estimates of DSW production would change by 50–100% depending on the assumptions used (e.g., Martin et al., 1998), and according to Yamamoto et al. (2002), the inversely estimated value of Itoh et al. (2003) could include a significant error due to the neglect of diapycnal mixing.

Sensitivity to the restoring time scale of the flux correction method is next examined. Fig. 11 shows the differences of salinity and potential temperature between the Tmix and FC30 cases at the same section as in Fig. 5. The difference is much smaller than that between the Ctrl and Tmix cases, although the decrease in restoring time scale leads to slight heating in the Okhotsk Sea and freshening around the Kuril Straits. Thus the simulation results are not so sensitive to the restoring time scale used, since the forcing is insensitive to the change in restoring time scale, at least in the range recommended by Barnier et al. (1995).

Although the slight difference between the Tmix and FC30 cases suggests a robustness of the results obtained in the previous sections, flux correction given under sea ice could affect the role of ice formation. This is particularly so for fresh water fluxes. The fresh water input due to the flux correction is thus compared with that due to ice formation, at the grids where ice is forming. In total, the input due to the restoring term was 25.5% of that due to ice formation and hence was not the main term. Moreover, both values are negative (i.e., increasing sea surface salinity), so that the restoring term did not reduce the effect of brine rejection. Although heat flux under sea ice could affect sea ice formation, the good agreement in ice production suggests that an error originating from this effect is insignificant. Hence, flux correction under sea ice did not lead to underestimate of the role of sea ice in DSW production.

7. Summary and discussion

In order to clarify the mechanisms responsible for the deep ventilation occurring in the Okhotsk Sea as compared with that in the North Pacific (e.g., Kitani, 1973), the effects of diapycnal mixing due to tidal mixing in the Kuril Straits and to double diffusion on ventilation of the Okhotsk Sea have been investigated through a set of experiments using an OGCM.

The results showed that the addition of (tidally-induced) diapycnal mixing in the Kuril Straits considerably enhances the ventilation of the Okhotsk Sea, whereas that of double diffusion does

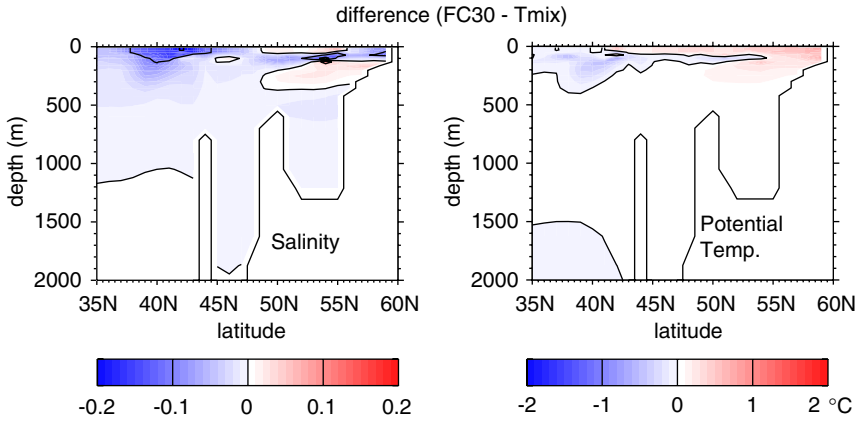

Fig. 11. Same as Fig. 6 but for the differences between the Tmix and FC30 cases.

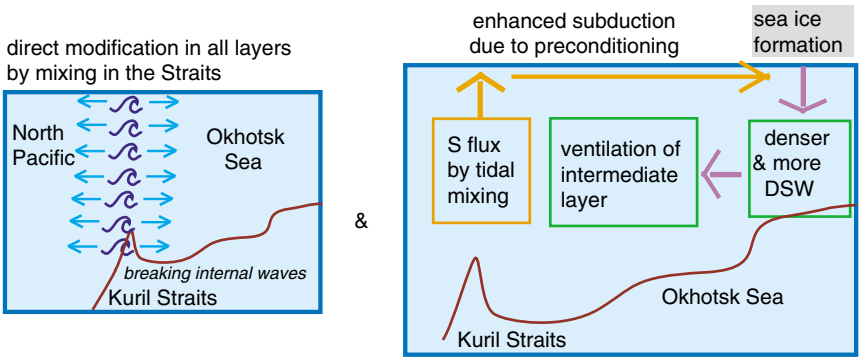

Fig. 12. Schematic view of the two roles of tidal mixing in the Kuril Straits in ventilation of the Okhotsk Sea.

not. Our analysis revealed that the tidal mixing exerts its influence through enhanced DSW production in the northern Okhotsk Sea in addition to the direct diapycnal mixing at the Kuril Straits as shown schematically in Fig. 12.

The mechanism of enhanced DSW production is identified as a preconditioning of salinity values in the northern shelf of the Okhotsk Sea. The preconditioning is due to the upward salt flux caused by tidal mixing from the saltier lower layer to the surface layer. The preconditioned (i.e., salted) water leads to increase in both density and production rate of the DSW when the winter cooling and sea-ice formation work in the northern Okhotsk Sea. The preconditioning also works to keep a mixture of subducted and surrounding waters at high salinity values, by increasing subsurface salinity values over the northern shelf of the Okhotsk Sea. As a result, the density and production rates of the DSW increase from $26.6\sigma_\theta$ and 0.01 Sv in the case without tidal mixing to $26.8\sigma_\theta$ and 0.13 Sv in the case with tidal mixing.

Previous studies of the DSW have so far overlooked the preconditioning due to tidal mixing and have focused only on the role of brine rejection. To bring out the importance of the preconditioning, the salinity increases due both to brine rejection and for DSW production are estimated. According to Gladyshev et al. (2000), who used in situ data that cover most of the shelf in the northern Okhotsk Sea and were taken in 1996 and 1997, the salinity increase due to brine rejection was less than 0.3 in most of the observation sites with the average of about 0.2, although the maximum value reached 0.8. (Here, the average is calculated from their estimates of the total salt production and the total volume of water influenced by brine.) Their estimate also suggested that even when the discussion is limited to DSW, a significant portion of the DSW also experienced salinity increases of less than 0.3.

The salinity increase required for DSW production can be estimated by adding a salinity difference between the DSW (33.3–33.5) and its source water (i.e., the EKCW near the sea surface, ~33.0) to a

possible salinity change in the Okhotsk Sea due to inflow of all of the fresh water and salt fluxes during spring to fall (except for that due to vertical mixing). Because of the large river runoff and excess precipitation over evaporation, the total flux would freshen the surface layer in the northern Okhotsk Sea by 0.2 on average, if vertical mixing is absent (the details are described in Appendix B and in Table 5). Thus, the required salinity increase is estimated to be 0.5–0.7. This value is significantly greater than the average salinity increase due to brine rejection.

Accordingly, if the estimate of Gladyshev et al. (2000) is appropriate for the climatology of the spatial average of the salinity increase due to brine rejection contributing to DSW production, there must be other sources that complement brine rejection. Our results suggest that one possible mechanism is the preconditioning of salinity values by tidal mixing. (Interestingly, the salt input through the Soya Strait is much less effective than river runoff or excess precipitation over evaporation (Appendix B), although it has been considered to be a major source in the salinity balance in the Okhotsk Sea (e.g., Talley and Nagata, 1995.)

However, Shcherbina et al. (2003) have recently shown that a salinity increase due to brine rejection reached 0.83 at one of the two mooring sites in 2000. This suggests that some uncertainty may be contained in the above estimates. Thus, an accurate estimate of the relative importance of the preconditioning by tidal mixing should await the future accumulation of observations. Nevertheless, broad agreement in the important features of the Okhotsk Sea vertical structure and circulation in the simulation and observations supports the possibility that the preconditioning by tidal mixing enhances DSW production. Also, observed high salinity anomalies in the upper layer around the Kuril Straits (Reid, 1973; Gladyshev, 1995) suggest that tidal mixing at the Kuril Straits makes a significant contribution as a preconditioning factor.

Table 5
Estimate of possible salinity change in the northern Okhotsk Sea

Component	Runoff	E-P	Melted ice	SWCW	Tatar Strait
δS	−0.17	−0.06	−0.04	+0.02	+0.03
S	0	0	3	34.0	16.5
V (10^3 km^3)	0.47	0.15	0.114	1.5	−0.16

δS is the possible salinity change in the northern Okhotsk Sea due to the corresponding flux component. S and V are respectively salinity and volume of water supplied from the corresponding flux components. A detailed description is given in Appendix B.

Associated with the enhanced DSW production, both freshening and cooling of an intermediate layer of the Okhotsk Sea occur, and thereby improve the simulated water masses in the Okhotsk Sea. In particular, a local PV minimum (in the vertical direction) is produced in the Okhotsk Sea around 300–500 m depth due to the enhanced DSW production. The reproduction of this feature is remarkable since it is a major characteristic feature of the OSMW. As far as we are aware, this is the first successful reproduction of such a local PV minimum in Okhotsk Sea water by an OGCM.

The diapycnal mixing in the Kuril Straits spreads freshening (or ventilation) to layers denser than the DSW, and down to $\sim 27.6\sigma_\theta$. This is consistent with the observational fact that the influence of the surface water properties is gradually carried down to such deep layers through diapycnal mixing (Wong et al., 1998), as mentioned in the introduction.

The direct effect of diapycnal mixing also enhances the freshening of the simulated intermediate water, including the DSW density layer. A quantitative estimate of the relative importance of the direct tidal mixing in the Kuril Straits and the DSW formation due to brine rejection in freshening of the OSMW is, however, beyond the scope of this study and awaits future observational studies. Nevertheless, because the vertical distribution of salinity around the Okhotsk Sea has a convex structure as a whole (i.e., $\partial^2 S/\partial z^2 < 0$; e.g., Watanabe and Wakatsuchi, 1998), the down-gradient type vertical diffusion acts to decrease salinity in the intermediate layer. Accordingly, the result that direct tidal mixing in the Kuril Straits can freshen the intermediate layer in the Okhotsk Sea should be robust in a qualitative sense. Also, an analysis of oxygen isotopes suggested that diapycnal mixing is important even above the 27.2 density layer (Yamamoto et al., 2002). Thus, it is likely that direct tidal mixing makes a significant contribution to freshening of the intermediate layer in the Okhotsk Sea.

Previous attempts to model the water masses in the Okhotsk Sea, such as the OSMW, and thus the NPIW have been unsatisfactory even though state-of-the-art OGCMs have been used (e.g, Yamanaka et al., 1998; Sakuma et al., 2003). Our results suggest that this is because the effect of diapycnal mixing process discussed so far has not been taken

into account through either a parameterization or explicit reproduction. Thus, attempts on the line of the present study could lead to better numerical simulations of the ventilation of intermediate water in both the Okhotsk Sea and the North Pacific.

Note that although increase of vertical mixing everywhere (not only locally) could also lead to a somewhat deeper ventilation due to downward diffusion, the location of enhanced mixing affects a ventilation process. This is particularly so for the case of the Kuril Straits. First, the Kuril Straits are the entrance of the Pacific water to the Okhotsk Sea. Such a location allows the effect of Kuril Strait mixing to spread in the Okhotsk Sea, leading to the enhanced DSW production. Interestingly, this means that enhanced mixing in the Kuril Straits induces enhanced sinking. In contrast, previous studies on global thermohaline circulation have shown that globally enhanced mixing induces enhanced upwelling from abyssal depths (through enhanced downward diffusion). The difference originates from the site of diapycnal mixing. The Kuril Straits are near a subduction region, whereas most of the global oceans are upwelling regions. Thus, the present result has an important implication not only for regional oceanography but also for an understanding of the role of diapycnal mixing in thermohaline circulation.

Second, the Kuril Straits are the exits of the water modified in the Okhotsk Sea and are directly adjacent to the waters of the North Pacific. This location enables the Kuril Strait mixing to affect the North Pacific. For example, fresher and colder water is supplied to the subsurface North Pacific in the Tmix case (Fig. 5). Also, the PV values in the upper layer are lowered (Fig. 5) by both the enhanced DSW production and the diapycnal mixing in the Kuril Straits. This lowering in PV strengthens the western boundary current of the subarctic gyre (the Oyashio, Figs. 2 and 3), since the isopycnal surfaces of the Oyashio deepen to the western boundary. Interestingly, the strengthened Oyashio crosses over the climatological zero-Sverdrup transport line to the subtropical gyre (Fig. 2). This cross-gyre boundary flow induces a transport of fresh, ventilated water from the Okhotsk Sea into the subtropical gyre, and hence affects ventilation of the subtropical North Pacific. Details of the mechanism and overall effect of the above process will be reported in another paper.

In addition, no observations have shown that it is the whole Okhotsk Sea where strong diapycnal mixing occurs. Rather, it is considered to occur locally. Among such mixing sites in the Okhotsk Sea, the Kuril Straits are special also in that locally enhanced diapycnal mixing occurs in such deep water (mixing occurs down to the $27.6\sigma_\theta$ density layer and up to the sea surface) (e.g., Yasuoka, 1968; Nakamura and Awaji, 2004). In contrast, although the shelf of the northern Okhotsk Sea is also suggested as a strong mixing site (e.g., Rogachev et al., 2001), it is too shallow to induce the observed deep indirect ventilation reaching to the $\sim 27.6\sigma_\theta$ density layer since the density over the shelf is $27.0\sigma_\theta$ at most (Gladyshev et al., 2000, 2003). Accordingly, diapycnal mixing in the Kuril Straits will have a different effect from that in other regions. Nevertheless, vertical mixing over the northern shelf may have important effects, for example, on heat exchange between ocean and atmosphere. Also, the northern shelf has a strong tidal flow (e.g., Nakamura et al., 2000a), and hence the effects of horizontal tidal motion may be important for the spreading and modification of DSW and the distribution and formation of sea ice. The investigation of these processes is remained for future works.

It should be noted that the model topography did not resolve all of the passages in the Kuril Straits and thus the detailed current field in this area. Nevertheless, the general features are captured in the simulations as discussed in Section 3. This is partly because we carefully prepared the model topography to include the two main straits (the Bussol and Kruzenshtern Straits), the shallow sills in the Kuril Straits, and the large islands near Hokkaido Island (e.g., Kunashiri Island). Also, the presence of many eddies and a strong tidal flow are reported around the Kuril Straits (e.g., Yasuda et al., 2000; Thomson et al., 1997). Some of the eddies arise from a tidal front around the Kuril Islands (Nakamura and Awaji, 2004). Although these cannot be resolved using the present model resolution, the effects of the eddies and tides were taken into consideration through the Gent and McWilliams' (1990) parameterization and through the increased vertical diffusion term, and lead to the general similarity to observation discussed in Section 3. Accordingly, although a much finer resolution model is needed in the future, the present model reasonably reproduced the observed flow field on a basin scale (the Okhotsk Sea scale) and hence supports a basic understanding of the role of tidal mixing in the Kuril Straits.

Acknowledgements

We appreciate the helpful comments of three anonymous reviewers. We also wish to acknowledge Dr. J.P. Matthews for his critical reading. This study is partly supported by the Category 7 of MEXT RR2002 Project for Sustainable Coexistence of Human, Nature and the Earth and by a Grant-in-Aid for the 21st Century COE Program (Kyoto University, G3). T.N. was also supported by the JSPS Research Fellowships for Young Scientists. Numerical calculations were done on the VPP800 at the Academic Center for Computing and Media Studies of Kyoto University.

Appendix A. Model description

The OGCM used in this study has been developed at Kyoto University (Ishikawa et al., 2002; Nakamura et al., 2003b; Toyoda et al., 2004), based on that developed in Meteorological Research Institute of Japan Meteorological Agency (Ishizaki, 1994), which is in turn based on Bryan (1969). The model solves the primitive equations with a free surface in spherical coordinates under Boussinesq and hydrostatic approximations and incorporates a sea ice model.

The horizontal grid system is a rectangular Arakawa staggered B grid (Bryan, 1969), and is basically the same as that of Modular Ocean Model (MOM) 3.0 developed at the Geophysical Fluid Dynamics Laboratory (GFDL/NOAA Department of Commerce). In the vertical, however, a hybrid system of the so called σ and z coordinates is used. The σ coordinate is adopted near the surface (above 60 m depth in the present case), in which the depths of discrete cells vary with time and space depending on sea surface height. Below the layer of σ coordinate, z coordinate is adopted, in which the partial cell scheme is used at the bottom in order to more accurately resolve the bottom topography. This hybrid system allows a very high resolution in the vertical near the surface even with a free surface and is thus useful for the improvement of surface mixed layer simulations (Toyoda et al., 2004). In both coordinates, vertical velocity and the other variables are staggered vertically as in MOM 3.0. Time integration of the prognostic equations is carried out by using mainly a centered leap-frog time stepping scheme with periodic application of Euler-backward scheme to handle the computational mode characteristic of a leap-frog scheme.

The momentum and continuity equations with a free surface are separated into the external and internal modes and are explicitly solved based on Killworth et al. (1991). The advection terms in the momentum equations are discretized using Takano–Oonishi scheme (Ishizaki and Motoi, 1999), which conserves both energy and pseudo enstrophy. The subgrid scale eddy viscosity is parameterized through bi-harmonic friction with Smagorinsky-like viscosity (Griffies and Hallberg, 2000). At the land boundary, no-normal flow is assumed. The bottom stress of the form $\rho_0 C_D |u_h|(u\cos\theta - \mathrm{sgn}(f)v\sin\theta, v\cos\theta + \mathrm{sgn}(f)u\sin\theta)$ is imposed at the bottom boundary, where C_D is a drag coefficient, θ is a rotation angle representing the effect of the bottom Ekman layer, and $\mathrm{sgn}(f)$ is the sign of the local Coriolis parameter. A no-slip condition is imposed at the lateral boundary.

The tracer equations, which predict potential temperature and salinity in the present study, adopt a third-order advection scheme (UTOPIA and QUICKEST; Hasumi and Suginohara, 1999) and incorporate isopycnal diffusion with eddy parameterization (Redi, 1982; Gent and McWilliams, 1990), together with a turbulence closure mixed layer scheme (Noh and Kim, 1999). Also, the effect of double diffusion is parameterized on the basis of Schmitt (1981) for the salt fingering condition and Fedorov (1988) for the diffusive convection condition, following Merryfield et al. (1999). In order to allow a large vertical diffusivity for unstably stratified water or the turbulence closure scheme, implicit time stepping is used for vertical mixing. At the land boundary, no tracer fluxes are assumed.

The equation of state used here is the international equation of state of seawater recommended by UNESCO (Millero et al., 1980; Millero and Poisson, 1981) but is written in terms of potential temperature following Jackett and McDougall (1995).

The sea ice model incorporated is a Hibler (1979) two-category ice model and is based on the works of Ikeda (1988, 1989a,b) and Ikeda et al. (1988). The main body of the ice is defined as thick ice. Thin ice can form in the open water portion of an ice-present model grid but is transformed into (or merges into) thick ice immediately. The prognostic variables are thus thickness, concentration, and velocity of the thick ice.

Ice velocity is calculated from simplified momentum equations which in the present version, include air-ice drag, ice-water drag, Coriolis force, gravity

associated with a sea surface slope, and viscosity which is retained for numerical stability, along with the local-acceleration and advection terms. The internal stresses are neglected although their effect is crudely taken into consideration through limiting the maximum value of ice thickness. Since model ice concentration is mostly less than 0.9 in the Okhotsk Sea with the present model resolution (Fig. 4), this simplification does not result in a significant change, although internal stresses should be included in a higher resolution model.

The thermodynamic equations contain atmospheric heat fluxes (shortwave and longwave radiation and sensible and latent heat fluxes) and a heat balance with the surface layer of the ocean model. An excess or shortage of heat in the ocean surface layer relative to the freezing point is immediately converted to decay or growth of ice. In this conversion, heat flux into an open water portion varies concentration through melting the thick ice or adding the thin ice from its side, while heat flux into the ice-covered portion varies thickness of the thick ice. A snow layer and heat storage of ice are neglected. The equations for ice volume (i.e., concentration times thickness) and concentration, which are integrated in time, are obtained from the combination of these thermodynamic effects and mass conservation for ice, together with kinematic conditions for ice thickness. (Diffusion of ice of small magnitude is added for numerical stability.)

Appendix B. An estimate of possible salinity changes in the northern Okhotsk Sea due to fresh water and salt fluxes

In order to evaluate the relative importance of the preconditioning due to tidal mixing in DSW formation, possible salinity changes due to the other fresh water and salt fluxes during spring to fall are estimated here.

For the estimate, a box model for the surface layer in the northern part of the Okhotsk Sea was considered, as shown in Fig. 13. The fluxes concerning salinity change in the box model are due to river runoff, excess precipitation over evaporation, melted ice, inflows of the SWCW and EKCW, outflows through the ESC and the Tatar Strait, and vertical mixing from below. (Ice formation does not matter here because of the choice of time duration.) Quantities associated with these flux components are hereafter indicated by the subscripts runoff, e − p, mice, swcw, ekcw, esc, ts, and vmix, respectively.

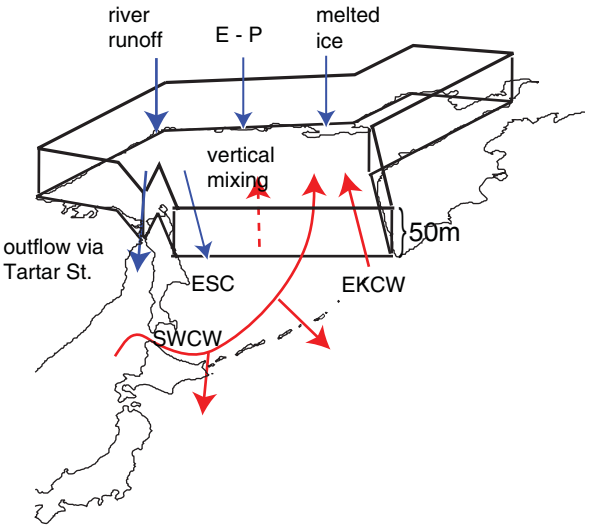

Fig. 13. Schematic of a box model for the surface layer in the northern Okhotsk Sea described in Appendix, which is superposed over coastlines around the Okhotsk Sea. (Runoff in reality enters through the side boundary but is presented by an arrow from above for simplicity.)

Suppose that the volume and salinity values of the box change from V_0 and S_0 to $V_0+\Delta V$ and $S_0+\Delta S$, respectively, due to the above flux components. Then the total change in amount of salt (ΔSalt) is,

$$\Delta\mathrm{Salt}=\rho_0[(S_0+\Delta S)(V_0+\Delta V)-S_0V_0], \qquad \text{(B.1)}$$

where the Boussinesq approximation is used with the reference density of $\rho_0\sim1.03\,\mathrm{g\,cm^{-3}}$. Thus, the estimation of ΔSalt and ΔV yields the resulting, possible salinity change ΔS.

The change of the box volume is given by

$$\Delta V=V_{\mathrm{runoff}}+V_{\mathrm{e-p}}+V_{\mathrm{mice}}+V_{\mathrm{swcw}}+V_{\mathrm{ekcw}}-V_{\mathrm{esc}}-V_{\mathrm{ts}}+V_{\mathrm{vmix}}. \qquad \text{(B.2)}$$

Here V_{runoff} is the volume supplied by runoff during spring to fall (here, April to December), and the other components are similarly defined. Note that precipitation over sea ice is not included because of the choice of the duration. The vertical volume transport due to an averaged vertical velocity is included in the volume change ΔV so that $V_{\mathrm{vmix}}=0$. The terms V_{esc} and V_{ekcw} include Ekman transport through the southern boundary of the box model for southward and northward components, respectively. Using these terms, the change of total

salt is given by

$$\Delta \mathrm{Salt}/\rho_0 = S_{\mathrm{runoff}} V_{\mathrm{runoff}} + S_{\mathrm{e-p}} V_{\mathrm{e-p}} + S_{\mathrm{mice}} V_{\mathrm{mice}} + S_{\mathrm{swcw}} V_{\mathrm{swcw}} + S_{\mathrm{ekcw}} V_{\mathrm{ekcw}} - S_{\mathrm{esc}} V_{\mathrm{esc}} - S_{\mathrm{ts}} V_{\mathrm{ts}} + \mathrm{Salt}_{\mathrm{vmix}}/\rho_0, \quad (B.3)$$

where S is salinity and $\mathrm{Salt}_{\mathrm{vmix}}$ is a salt input due to vertical mixing.

The initial value of salinity is set as $S_0 = S_{\mathrm{ekcw}}$ to focus on the salinity modification in the Okhotsk Sea. In calculation of the initial box volume, the initial depth of the box is set to be 50 m to consider salinity change of a mixed layer just before winter, and the latitude of the southern boundary is set at 51 °N. In addition, the salinity of the outflowing ESC is assumed to be the same as the final value ($S_{\mathrm{esc}} = S_0 + \Delta S$) to avoid the difficulty of determining its representative value. This may lead to an underestimate of the possible salinity change since the outflow would first export water of the initial salinity.

Substituting (B.2) and (B.3) into (B.1) and using the above assumptions, the change in salinity becomes

$$\Delta S = \delta S_{\mathrm{runoff}} + \delta S_{\mathrm{e-p}} + \delta S_{\mathrm{mice}} + \delta S_{\mathrm{swcw}} + \delta S_{\mathrm{ts}} + \delta S_{\mathrm{vmix}}, \quad (B.4)$$

$$\delta S_\phi = \frac{(S_\phi - S_0) V_\phi}{V_0 + \Delta V + V_{\mathrm{esc}}}, \quad (B.5)$$

where δS_ϕ represents a contribution from each flux component and the subscript ϕ be replaced by the corresponding subscript. (The last term in (B.4) is defined as $\delta S_{\mathrm{vmix}} = \mathrm{Salt}_{\mathrm{vmix}}/[\rho_0(V_0 + \Delta V + V_{\mathrm{esc}})]$.)

Estimate of each contribution in (B.4) was then obtained as follows (Table 5). Salinity of river runoff and excess precipitation over evaporation is neglected ($S_{\mathrm{runoff}} = S_{\mathrm{e-p}} = 0$), and their volumes are based on Talley and Nagata (1995) and the OMIP data set (Röske, 2001), respectively. The salinity of the water derived from melted ice is set to that of sea ice, which in turn is set to 3. For the volume estimate of melted ice, a half of the produced ice is assumed to melt in the northern Okhotsk Sea (i.e., the other half is assumed to drift away to or be produced in the southern region). The ice production used is the 12-year average value (Alfultis and Martin, 1987; Martin et al., 1998; Gladyshev et al., 2000). The salinity of the SWCW is approximated as 34.0 based on Takizawa (1982). The volume of the SWCW that flows into the Okhotsk Sea during spring to fall is estimated to be 0.5 Sv on average (Aota, 1975), and then $\frac{1}{8}$ of this volume is assumed to enter the box, on the assumption that a half of the SWCW mixes with Okhotsk Sea water before flowing out to the Pacific, and that a half of the subsequent mixture reaches the northern Okhotsk Sea with a half of it present in the upper 50 m layer. The salinity of the water flowing out through the Tatar Strait is approximated as a half of the initial value in the interior ($S_0/2 = 16.5$), considering that the sea surface salinity around the strait is less than 20 (Fujii and Abe, 1976; Gladyshev et al., 2003) and that the true value would lie somewhere between 0 and S_0. Its volume is assumed to be a half of the runoff from the Amur river because we are not aware of any available observations, and because the volume should be less than the Amur river runoff, so that the effect of the runoff spreads into the Okhotsk Sea as in the observations though the Amur river is located near the Tatar Strait. The initial salinity is set to be $S_0 = 33.0$ and the initial box volume is estimated as $V_0 \sim 4 \times 10^4\,\mathrm{km}^3$, approximating the area to $\sim 86\,\mathrm{km}^2$. Finally, the other terms in the denominator in (B.5) become

$$\Delta V + V_{\mathrm{esc}} = V_{\mathrm{runoff}} + V_{\mathrm{e-p}} + V_{\mathrm{mice}} + V_{\mathrm{swcw}} + V_{\mathrm{ekcw}} - V_{\mathrm{ts}}.$$

The right-hand side can be approximated by V_{ekcw}, which in turn is approximated by V_{esc}. This is because the terms V_{ekcw} and V_{esc} are predominant in (B.2) (other terms are smaller than an error in estimating V_{esc}). To estimate V_{esc}, ESC volume transport in the surface layer is approximated as 2 Sv. This value corresponds to the total transport of the model ESC and to $\frac{1}{2} - \frac{1}{4}$ of the observed total transport (Ohshima et al., 2002), so that it may be an overestimate, leading to an underestimate of the possible salinity change.

According to the estimates shown in Table 5, the net flux (except for vertical mixing) works to decrease the surface layer salinity in the northern Okhotsk Sea by 0.2 during spring to fall. It should be noted that these estimates may contain errors, although it is difficult to estimate the magnitudes of errors because, as far as we are aware, not only true values but also ranges of errors (or interannual variations) in the observational values used here are not available in a climatological sense. Since some unknown values are chosen so that they would lie between the maximum and the minimum possible values, each estimate of δS could have an error of

~100% at the maximum. Nevertheless, as long as the order of each estimates is relevant, the dominance of a runoff effect would ensure a robust nature of the results. Thus, the total error depends mainly on an estimate of runoff.

References

Aota, M., 1975. Studies on the Soya Warm Current. Teion Kagaku 33, 151–172 (in Japanese).

Aota, M., Kawamura, T., 1978. Observation of oceanographic condition in the Okhotsk Sea coast of Hokkaido in winter. Teion Kagaku, 33 (in Japanese).

Alfultis, M.A., Martin, S., 1987. Satellite passive microwave studies of the Sea of Okhotsk Sea ice cover and its relation to oceanic processes. Journal of Geophysics Research 92, 13,013–13,028.

Awaji, T., Masuda, S., Ishikawa, Y., Sugiura, N., Toyoda, T., Nakamura, T., 2003. State estimation of the North Pacific Ocean by a four-dimensional variational data assimilation. Journal of Oceanography 59, 931–943.

Barnier, B., Siefridt, L., Marchesiello, P., 1995. Thermal forcing for a global ocean circulation model using a three-year climatology of ECMWF analyses. Journal of Marine Systems 6, 363–380.

Bryan, K., 1969. A numerical method for the study of the circulation of the World Ocean. Journal of Computational Physics 4, 347–376.

Cavalieri, D., Gloerson, P., Zwally, J., 2002. In: Maslanik, J., Stroeve J. (Eds.), Near Real-Time DMSP SSM/I Daily Polar Gridded Sea Ice Concentrations. National Snow and Ice Data Center, Boulder, CO (Digital media, updated regularly).

da Silva, A.M., Young, C.C., Levitus, S., 1994. Atlas of Surface Marine Data 1994, vol. 1, Algorithms and Procedures, NOAA Atlas NESDIS 6, U.S. Department of Commerce, Washington, DC, 83pp.

Favorite, F., Dodimead, A.J., Nasu, K., 1976. Oceanography of the Subarctic Pacific region, 1960–1971. Bulletin of International North Pacific Fishing Community 33, 187pp.

Fedorov, K.N., 1988. Layer thicknesses and effective diffusivities in "diffusive" thermohaline convection in the ocean. In: Nihoul, J.C.J., Jamart, B.M. (Eds.), Small-Scale Turbulence and Mixing in the Ocean. Ess, Elsevier, pp. 471–479.

Fetterer, F., Knowles, K., 2002. Sea Ice Index. National Snow and Ice Data Center, Boulder, CO (Digital media, available from its web site).

Freeland, H.J., Bychkov, A.S., Whitney, F., Taylor, C., Wong, C.S., Yurasov, G.I., 1998. WOCE section P1W in the Sea of Okhotsk-1. Oceanographic data description. Journal of Geophysical Research 103, 15, 613–15, 623.

Fujii, K., Abe, M., 1976. Preliminary report on the water masses appeared in summer in the western region of the Okhotsk Sea. Bulletin of the Hokkaido Regional Fisheries Research Laboratary 41, 93–117 (in Japanese).

Gent, P.R., McWilliams, J.C., 1990. Isopycnal mixing in ocean circulation models. Journal of Physical Oceanography 20, 150–155.

Gladyshev, S.V., 1995. Fronts in the Kuril Island region. Oceanology 34, 452–459 (English translation).

Gladyshev, S., Martin, S., Riser, S., Figurkin, A., 2000. Dense water production on the northern Okhotsk shelves: comparison of ship-based spring-summer observations for 1996 and 1997 with satellite observations. Journal of Geophysical Research 105, 26,281–26,299.

Gladyshev, S., Talley, L., Kantakov, G., Khen, G., Wakatsuchi, M., 2003. Distribution, formation, and seasonal variability of Okhotsk Sea Mode Water. Journal of Geophysical Research 108, 3186.

Griffies, S.M., Hallberg, R.W., 2000. Biharmonic friction with a Smagorinsky-like viscosity for use in large-scale eddy-permitting ocean models. Monthly Weather Review 128, 2935–2946.

Hasumi, H., Suginohara, N., 1999. Sensitivity of a global ocean general circulation model to tracer advection schemes. Journal of Physical Oceanography 29, 2730–2740.

Hibiya, T., Ogasawara, M., Niwa, Y., 1998. A numerical study of the fortnightly modulation of basin-ocean water exchange across a tidal mixing zone. Journal of Physical Oceanography 28, 1224–1235.

Hibler, W.D., 1979. A dynamic thermodynamic sea ice model. Journal of Physical Oceanography 9, 815–845.

Ikeda, M., 1988. A three-dimensional coupled ice-ocean model of coastal circulation. Journal of Geophysical Research 93, 10,731–10,748.

Ikeda, M., 1989a. A coupled ice-ocean mixed layer model of the marginal ice zone to wind forcing. Journal of Geophysical Research 94, 9699–9709.

Ikeda, M., 1989b. Snow cover detected by diurnal warming of sea ice/snow surface off Labrador in NOAA imagery. IEEE Transactions of Geoscience and Remote Sensing 27, 552–560.

Ikeda, M., Yao, T., Symonds, G., 1988. Simulated fluctuation in annual Labrador Sea-ice cover. Atmosphere Ocean 26, 16–39.

Ishizaki, H., 1994. A simulation of the abyssal circulation in the North Pacific Ocean. Part I: flow field and comparison with observations. Journal of Physical Oceanography 24, 1921–1939.

Ishizaki, H., Motoi, T., 1999. Reevaluation of the Takano-Oonishi scheme for momentum advection on bottom relief in ocean models. Journal of Atmospheric and Oceanic Technology 16, 1994–2010.

Ishikawa, Y., Awaji, T., Toyoda, T., Komori, N., 2002. Construction of a data assimilation system for ocean general circulations—Determination of weight parameters for the adjoint method—Proceedings of International Symposium, En route to GODAE, B09-21, Biarritz, France.

Itoh, M., Ohshima, K.I., Wakatsuchi, M., 2003. Distribution and formation of Okhotsk Sea Intermediate Water: an analysis of isopycnal climatological data. Journal of Geophysical Research 108, 3258.

Jackett, D.R., McDougall, T.J., 1995. Minimal adjustment of hydrographic profiles to achieve static stability. Journal of Atmosphere and Ocean Technology 12, 381–389.

Japan Meteorological Agency, 2003. Kaihyo-Gaiho (in Japanese, available on the website of Sapporo District Meteorological Observatory), 5.

Katsumata, K., Ohshima, K.I., Kono, T., Itoh, M., Yasuda, I., Volkov, Y.N., Wakatsuchi, M., 2004. Water exchange and tidal currents through the Bussol' Strait revealed by direct current measurements. Journal of Geophysical Research 109, C09S06, doi:10.1029/2003JC001864.

Kawasaki, Y., 1996. The origin of the North Pacific Intermediate Water—from the observations in the Okhotsk Sea—. Kaiyo Monthly 28, 545–552 (in Japanese).

Kawasaki, Y., Kono, T., 1994. Distribution and transport of Subarctic Waters around the middle of Kuril Islands. Umi to Sora 70, 71–84 (in Japanese with English abstract and figure captions).

Killworth, P.D., Stainforth, D., Webb, D.J., Paterson, S.M., 1991. The development of a free-surface Bryan-Cox-Semtner ocean model. Journal of Physical Oceanography 21, 1333–1348.

Kitani, K., 1973. An oceanographic study of the Okhotsk Sea—particularly in regard to cold waters. Bulletin of the Far Seas Fisheries Research Laboratory 9, 45–77.

Kono, T., Kawasaki, Y., 1997. Results of CTD and mooring observations southeast of Hokkaido 1. Annual velocity and transport variations in the Oyashio. Bulletin of the Hokkaido National Fisheries Research Institute 61, 65–81.

Levitus, S., Boyer, T.P., 1994. World Ocean Atlas 1994, vol. 4, Temperature. NOAA Atlas NESDIS 4, U.S. Govt. Print. Off., Washington, DC, 117pp.

Levitus, S., Burgett, R., Boyer, T.P., 1994. World Ocean Atlas 1994, vol. 3, Salinity. NOAA Atlas NESDIS 3, U.S. Govt. Print. Off., Washington, DC, 99pp.

Martin, S., Drucker, R., Yamashita, K., 1998. The production of ice and dense shelf water in the Okhotsk Sea polynyas. Journal of Geophysical Research 103, 27,771–27,782.

Matsuyama, M., Aota, M., Ogasawara, I., Matsuyama, S., 1999. Seasonal variation of Soya Warm Current. Umi no Kenkyu 8, 333–338 (in Japanese with English abstract).

Merryfield, W.J., Holloway, G., Gargett, A.E., 1999. A global ocean model with double-diffusive mixing. Journal of Physical Oceanography 29, 1124–1142.

Millero, F.J., Poisson, A., 1981. International one-atmosphere equation of state for sea water. Deep-Sea Research, 28A, 625–629.

Millero, F.J., Chen, C.-T., Bradshaw, A., Schleicher, K., 1980. A new high pressure equation of state for sea water. Deep-Sea Research, 27A, 255–264.

Mizuta, G., Fukamachi, Y., Ohshima, K.I., Wakatsuchi, M., 2003. Structure and Seasonal variability of the East Sakhalin Current. Journal of Physical Oceanography 33, 2430–2445.

Moroshkin, K.V., 1966. Water masses of the Sea of Okhotsk, Joint Publ. Res. Serv. 43942, U.S. Department of Commerce, Washington, DC, 98pp.

Nakamura, T., Awaji, T., 2001. A growth mechanism for topographic internal waves generated by an oscillatory flow. Journal of Physical Oceanography 31, 2511–2524.

Nakamura, T., Awaji, T., Hatayama, T., Akitomo, K., Takizawa, T., 2000a. Tidal exchange through the Kuril Straits. Journal of Physical Oceanography 30, 1622–1644.

Nakamura, T., Awaji, T., Hatayama, K., Akitomo, T., Takizawa, T., Kono, Y., Kawasaki, M., Fukasawa, 2000b. The generation of large-amplitude unsteady lee waves by subinertial K_1 tidal flow: a possible vertical mixing mechanism in the Kuril Straits. Journal of Physical Oceanography 30, 1601–1621.

Nakamura, T., Awaji, T., 2004. Tidally-induced diapycnal mixing in the Kuril Straits and its role in water transformation and transport: a three-dimensional nonhydrostatic model experiment. Journal of Geophysical Research 109, C09S07.

Nakamura, T., Awaji, T., Toyoda, T., Ishikawa, Y., 2003a. Coastal Oyashio in a North Pacific simulation experiment. Bulletin on Coastal Oceanography 41, 13–22.

Nakamura, T., Toyoda, T., Ishikawa, Y., Konda, M., Awaji, T., Takizawa, T., In, T., 2003b. Tidal processes in the Kuril Straits and their effects on the North Pacific. Kaiyo Monthly 41, 13–22 (in Japanese).

Nakamura, T., Toyoda, T., Ishikawa, Y., Awaji, T., 2006. The effects of tidal mixing at the Kuril Straits on North Pacific ventilation: adjustment of the intermediate layer revealed from numerical experiments. Journal of Geophysical Research, 2003, in press.

Noh, Y., Kim, H.J., 1999. Simulations of temperature and turbulence structure of the oceanic boundary layer with the improved near-surface process. Journal of Geophysical Research 104, 15,621–15,634.

Ohshima, K.I., Wakatsuchi, M., Fukamachi, Y., Mizuta, G., 2002. Near-surface circulation and tidal currents of the Okhotsk Sea observed with the satellite-tracked drifters. Journal of Geophysical Research 107, NO. C11, 3195, doi:10.1029/2001JC001005.

Overland, J.E., Spillane, M.C., Hurlburt, H.E., Wallcraft, J., 1994. A numerical study of the circulation of the Bering Sea Basin and exchange with the North Pacific Ocean. Journal of Physical Oceanography 24, 736–758.

Redi, M.H., 1982. Oceanic isopycnal mixing by coordinate rotation. Journal of Physical Oceanography 12, 1154–1158.

Reid, J.L., 1973. North Pacific Ocean Waters in Winter. The Johns Hopkins Press, Baltimore, 85pp.

Riser, S.C., 2001. The exchange of water between the Okhotsk Sea and the North Pacific Ocean, and implications of intermediate water formation. Proceedings of International Symposium on Atmosphere-Ocean-Cryosphere Interaction in the Sea of Okhotsk and the Surrounding Environment 2–3. Hokkaido University, Sapporo, Japan.

Rogachev, K.A., Carmack, E.C., Salomatin, A.S., Alexanina, M.G., 2001. Lunar fortnightly modulation of tidal mixing near Kashevarov Bank, Sea of Okhotsk, and its impact on biota and sea ice. Progress in Oceanography 49, 373–390.

Röske, F., 2001. An atlas of surface fluxes based on the ECMWF re-analysis—a climatological dataset of force global ocean general circulation models. Max-Planck-Institut fü Meteorologie 323, 26pp.

Sakuma, H., Sasaki, H., Takahashi, K., Kagimoto, T., Yamagata, T., Sato, T., 2003. Global Eddy-resolving simulation by the Earth simulator: brief report on the first run. Proceedings of Recent Advances in Marine Science and Technology 2002, PACON International.

Schmitt, R.W., 1981. Form of the temperature-salinity relationship in the central water: evidence for double-diffusive mixing. Journal of Physical Oceanography 11, 1015–1026.

Shcherbina, A.Y., Talley, L.D., Rudnick, D.L., 2003. Direct observations of North Pacific ventilation: Brine rejection in the Okhotsk Sea. Science 302, 1952–1955.

Sekine, Y., 1990. A barotropic numerical model for the wind-driven circulation in the Okhotsk Sea. Bulletin of Bioresearch Mie University 3, 25–39.

Shiller, A., Godfrey, J.S., McIntosh, P.C., Meyers, G., Wijffels, S.E., 1998. Seasonal near-surface dynamics and thermodynamics of the Indian Ocean and Indonesian Throughflow in a global ocean general circulation model. Journal of Physical Oceanography 28, 2288–2311.

Shimizu, D., Ohshima, K.I., 2002. Barotropic response of the Sea of Okhotsk to wind forcing. Journal of Oceanography 58, 851–860.

Sverdrup, H., Johnson, M., Fleming, R., 1942. The Oceans, Prentice-Hall, Englewood Cliffs, NJ, 1087pp.

Takizawa, T., 1982. Characteristics of the Soya Warm Current in the Okhotsk Sea. Journal of Oceanography Society of Japan 38, 281–292.

Talley, L.D., 1991. An Okhotsk Sea water anomaly: implications for ventilation in the North Pacific. Deep-Sea Research 38, s171–190.

Talley, L.D., 1993. Distribution and formation of North Pacific intermediate water. Journal of Physical Oceanography 23, 517–537.

Talley, L.D., Nagata, Y., 1995. The Okhotsk Sea and Oyashio region. PICES Scientific Report No. 2, Sidney, B.C., Canada, 227pp.

Thomson, R.E., LeBlond, P.H., Rabinovich, A.B., 1997. Oceanic odyssey of a satellite-tracked drifter: North Pacific variability delineated by a single drifter trajectory. Journal of Oceanography 53, 81–87.

Toyoda, T., Awaji, T., Ishikawa, Y., Nakamura, T., 2004. Preconditioning of winter mixed layer in the formation of North Pacific eastern subtropical mode water. Geophysical Research Letters 31, L17206.

Uda, M., 1963. Oceanography of the Subarctic Pacific Ocean. Journal of Fisheries Research Board Canada 20, 119–179.

Wakatsuchi, M., Martin, S., 1991. Water circulation of the Kuril Basin of the Okhotsk Sea and its relation to eddy formation. Journal of Oceanography Society of Japan 47, 152–168.

Warner, M.J., Bullister, J.L., Wisegraver, D.P., Gammon, R.H., Weiss, R.F., 1996. Basin-wide distributions of chlorofluorocarbons CFC-11 and CFC-12 in the North Pacific. Journal of Geophysical Research 101, 20,525–20,542.

Watanabe, T., Wakatsuchi, M., 1998. Formation of $26.8\sigma_\theta$ water in the Kuril Basin of the Sea of Okhotsk as a possible origin of North Pacific Intermediate Water. Journal of Geophysical Research 103, 2849–2865.

Weaver, A.J., Hughes, T.M.C., 1996. On the incompatibility of ocean and atmosphere models and the need for flux adjustments. Climate Dynamics 12, 141–170.

Wong, C.S., Matear, R.J., Freeland, H.J., Whitney, F.A., Bychkov, A.S., 1998. WOCE line P1W in the Sea of Okhotsk 2. CFCs and the formation rate of intermediate water. Journal of Geophysical Research 103, 15,625–15,642.

Yamamoto, M., Watanabe, S., Tsunogai, S., Wakatsuchi, M., 2002. Effects of sea ice formation and diapycnal mixing on the Okhotsk Sea Intermediate Water clarified with oxygen isotopes. Deep-Sea Research I 49, 1165–1174.

Yamanaka, G., Kitamura, Y., Endoh, M., 1998. Formation of North Pacific Intermediate Water in Meteorological Research Institute ocean general circulation model 1. Subgrid-scale mixing and marginal sea fresh water. Journal of Geophysical Research 103, 30,885–30,903.

Yamanaka, Y., Tajika, E., 1996. The role of the vertical fluxes of particulate organic matter and calcite in the oceanic carbon cycle: studies using biogeochemical general circulation model. Global Biogeochemistry Cycles 10, 361–382.

Yasuda, I., 1997. The origin of the North Pacific intermediate water. Journal of Geophysical Research 102, 893–910.

Yasuda, I., Okuda, K., Shimizu, Y., 1996. Distribution and formation of North Pacific Intermediate Water in the Kuroshio-Oyashio interfrontal zone. Journal of Physical Oceanography 26, 448–465.

Yasuda, I., Ito, S.I., Shimizu, Y., Ichikawa, K., Ueda, K.I., Honma, T., Uchiyama, M., Watanabe, K., Sunou, N., Tanaka, K., Koizumi, K., 2000. Cold-core anticyclonic eddies south of the Bussol' Strait in the Northwestern Subarctic Pacific. Journal of Physical Oceanography 30, 1137–1157.

Yasuda, I., Hiroe, Y., Komatsu, K., Kawasaki, K., Joyce, T.M., Bahr, F., Kawasaki, Y., 2001. Hydrographic structure and transport of the Oyashio south of Hokkaido and the formation of North Pacific Intermediate Water. Journal of Geophysical Research 106, 6931–6942.

Yasuda, I., Kouketsu, S., Katsumata, K., Ohiwa, M., Kawasaki, Y., Kusaka, A., 2002. Influence of Okhotsk Sea Intermediate Water on the Oyashio and North Pacific Intermediate Water. Journal of Geophysical Research 107, 3237.

Yasuoka, T., 1968. Hydrography in the Okhotsk Sea-(2). The Oceanographical Magazine 20, 55–63.

You, Y., Suginohara, N., Fukasawa, M., Yasuda, I., Kaneko, I., Yoritaka, H., Kawamiya, M., 2000. Roles of the Okhotsk Sea and Gulf of Alaska in forming the North Pacific Intermediate Water. Journal of Geophysical Research 105, 3253–3280.

Zhang, J., Schmitt, R.W., Huang, R.X., 1998. Sensitivity of the GFDL Modular Ocean Model to parameterization of double-diffusive processes. Journal of Physical Oceanography 28, 589–605.